

SignX: Continuous Sign Recognition in Compact Pose-Rich Latent Space

Sen Fang¹, Yalin Feng^{2*}, Chunyu Sui³, Hongbin Zhong⁴, Hongwei Yi⁵, Dimitris N. Metaxas¹

¹Rutgers University, ²Nanyang Technological University, ³Columbia University,

⁴Georgia Institute of Technology, ⁵Max Planck Institute for Intelligent Systems

<https://SignerX.github.io/SignX/>

Abstract

The complexity of sign language data processing brings many challenges. The current approach to recognition of ASL signs aims to translate RGB sign language videos through pose information into English-based ID Glosses, which serve to uniquely identify ASL signs¹. This paper proposes **SignX**, a novel framework for continuous sign language recognition in compact pose-rich latent space. First, we construct a unified latent representation that encodes heterogeneous pose formats (SMPLer-X, DWPose, Mediapipe, PrimeDepth, and Sapiens Segmentation) into a compact, information-dense space. Second, we train a ViT-based Video2Pose module to extract this latent representation directly from raw videos. Finally, we develop a temporal modeling and sequence refinement method that operates entirely in this latent space. This multi-stage design achieves end-to-end sign language recognition while significantly reducing computational consumption. Experimental results demonstrate that SignX achieves state-of-the-art accuracy on continuous sign language recognition.

1 Introduction

Sign Language Recognition (SLR) aims to automatically convert sign language videos into text or glosses (represented as upper-case text, which serve as unique identifiers of signs). It has important social value in facilitating barrier-free communication between deaf and hearing individuals (Camgöz et al., 2018; Cihan Camgöz et al., 2020; Stoll et al., 2020; Yin et al., 2021). However, SLR faces technical challenges: (1) *Signed languages are complex multimodal movements*, involving hand and arm movements as well as facial expressions and body postures, with complex temporal dependencies among these modalities (Boháček

*Equal Contribution.

¹Note that there is no shared convention for assigning such glosses to ASL signs, so consistent glossing conventions must be used across all datasets.

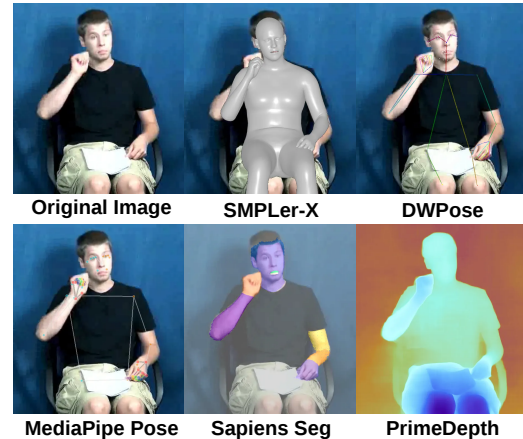


Figure 1: **Multimodal pose estimation methods:** SMPLer-X (Cai et al., 2023) can provide accurate 3D human body parameters; DWPose (Yang et al., 2023) focuses on real-time 2D keypoint detection; Mediapipe (Lugaresi et al., 2019) provides lightweight but efficient 3D pose prediction; PrimeDepth (Zavadski et al., 2024) can obtain scene depth information; while Sapiens Segmentation (Khirodkar et al., 2024) provides fine-grained human body part segmentation results. These methods each have their own characteristics, providing rich feature representations for sign language recognition.

and Hruz, 2022; Vintar et al., 2012; Von Agris and Kraiss, 2010). (2) *Existing SL datasets are limited in size and lack a uniform preprocessing format*, with complicated processing pipelines, which severely constrains the application of deep learning methods (Duarte et al., 2021b; Rayner et al., 2016; Cihan Camgöz et al., 2020). (3) *Different pose processing formats attend to different visual aspects, leading to distributional shifts that limit effective integration* of innovative advantages across model types (Fang et al., 2025a,c).

To address these challenges, we develop a *Vid2Pose module* by using a novelty ViT model (Dosovitskiy et al., 2021), which inspired by the five most powerful pose estimation models. As shown in Fig. 1, we learn the Vid2Pose process in the encoder of the ViT model through a unified pose representation. Specifically, SMPLer-X (Cai et al.,

2023) provides 3D body mesh with kinematic and pose parameters for modeling body dynamics; DW-Pose (Yang et al., 2023) captures 2D keypoints with rich facial landmarks essential for grammatical expressions; MediaPipe (Lugaresi et al., 2019) offers 3D joint coordinates that represent overall body motion trends. Additionally, PrimeDepth (Zavadski et al., 2024) provides spatial depth information for disambiguating front-back positioning, while Sapiens Segmentation (Khirodkar et al., 2024) captures human body shape through fine-grained part boundaries. This complementary design captures not only hand movements but also fine-grained details such as *body dynamics, facial expressions, motion trajectories, spatial depth, and body shape*, with the goal of fully capturing a person’s pose (Saunders et al., 2020b; Stoll et al., 2020; Moryossef, 2022). This end-to-end processing approach greatly simplifies the *pose representation* (Boháček and Hružík, 2022; Cho et al., 2021; Chiang et al., 2019) process that is necessary for SL recognition.

Then we employ the *Pose2Gloss method* to identify the pose features in the latent space, but most existing recognition models have several limitations: (1) Most are based on *raw pose data learning*, which is inconvenient in practical applications and requires assistance from other pose information extraction models (Wang et al., 2018a,b). (2) Furthermore, models capable of real-time translation have *low accuracy*, while highly accurate models have *slow output speeds* (Saunders et al., 2021b). (3) Even purely pixel-space-based models are limited by *high computational costs*, and their attention mechanisms cannot support higher performance ceilings for longer and more accurate translations (Cui et al., 2017; Koller, 2020; Lapiak; Zelinka and Kanis, 2020b).

To address these limitations, we develop a recognition framework that operates entirely in the compact pose-rich latent space. Starting from the 2048-dimensional pose features extracted by Vid2Pose, we employ a ResNet34 backbone (He et al., 2016) followed by TemporalConv layers (Lea et al., 2016) to capture hierarchical temporal patterns. These are jointly learned with the pose features. To refine these predictions into coherent sequences, we apply a Transformer-based encoder-decoder (Zhang et al., 2023a) that performs sequence-to-sequence refinement with beam search and CTC regularization (Cihan Camgöz et al., 2020; Vaswani et al., 2017). This design achieves accurate recognition directly in latent space, eliminating the need for

raw pose processing and reducing computational overhead compared to vision-based approaches.

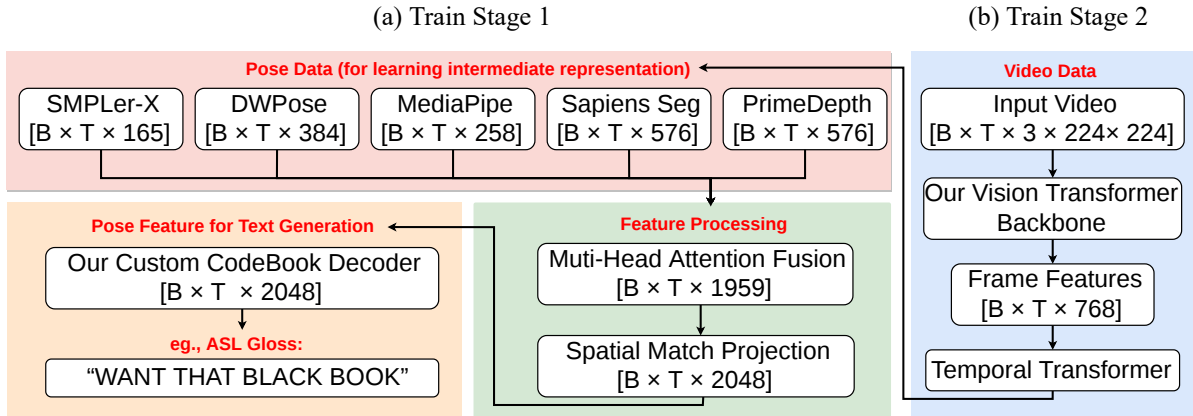
Through this multi-stage training, SignX achieves powerful functionality while maintaining architectural simplicity: It learns from various formats of prior knowledge and can directly use the raw video as input. Experimental results show that SignX achieves good performance on our ASL and mainstream datasets (Neidle and Metaxas, 2025; Forster et al., 2012; Zhou et al., 2021a; Li et al., 2020a), surpassing existing methods in both accuracy and robustness (Chen et al., 2023).

The main contributions of this paper can be summarized in the following three points:

- We propose **SignX**, a novel framework for continuous sign language recognition that operates in a **compact pose-rich latent space**, unifying heterogeneous pose representations from five powerful estimation methods into a single information-dense encoding.
- We develop a **ViT-based Vid2Pose module** that extracts unified pose representations (encompassing facial expressions, body dynamics, motion trajectories, spatial depth, and body shape) directly from raw videos in an end-to-end manner, eliminating the need for explicit pose estimation pipelines and significantly simplifying the workflow.
- We design a **latent-space recognition method** that combines ResNet temporal modeling with **Transformer-based sequence refinement**, achieving accurate sign recognition while reducing computational overhead compared to pixel-space approaches.

2 Related Work

Sign Recognition and Diffusion Models. While traditional SLR frameworks predominantly rely on feature extraction from high-dimensional pixel streams or raw skeletal coordinates, these approaches are often hindered by data noise and the difficulty of capturing fine-grained grammatical nuances. In contrast, diffusion models have recently redefined sign language generation by operating within compressed, structured latent spaces (Fang et al., 2025b,a). Departing from existing SLR paradigms, our work introduces a **novel recognition framework that performs inference directly within a sign-specific latent space**. Inspired by



B: batch size T: frame count Pose Inputs: the file that stores pose information through various tools, RGB-D is a one-dimensional array

Figure 2: **Overview of Constructing Compact Pose-Rich Latent Space:** Overall, we utilize ViT (Dosovitskiy et al., 2021) to construct and accommodate a pose latent space. It has two entry points: a video entry at the top layer and a pose data entry in the middle section. (a) For training stage 1, we first train the pose fusion layer to output simple text information, ensuring that the learned pose representations are meaningful. (b) For training stage 2, we freeze all other components and only learn how RGB videos can be correctly converted into our pose features. For inference, only RGB is used as input, so we must ensure that we can encode RGB inputs into our pose features.

the high-efficiency latent modeling in diffusion processes (Rombach et al., 2021; Fang et al., 2025d), we leverage a pose-rich latent domain to bypass the limitations of raw data processing. This shift allows our model to more effectively capture complex spatiotemporal dependencies and linguistic structures, establishing a new direction for robust and efficient American Sign Language recognition.

3 Compact Pose-Rich Latent Space

3.1 Data Processing

To address the challenge of integrating heterogeneous pose information for SL recognition, we first construct a comprehensive processing pipeline that standardizes multiple pose formats. First, we use a high-quality ASLLRP SignStream® 3 Corpus (Neidle et al., 2022a; Neidle and Metaxas, 2025) dataset, which contains over 80 hours of American Sign Language (ASL) videos with synchronized front view, side view, and facial close-up recordings. For each input video $V \in \mathbb{R}^{T \times H \times W \times 3}$, where T represents the number of frames and H, W represent height and width, respectively, we extract sequential pose representations for each pose type: $P_{\text{DWPose}} \in \mathbb{R}^{T \times 384}$, $P_{\text{MediaPipe}} \in \mathbb{R}^{T \times 258}$, $P_{\text{SMPLer-X}} \in \mathbb{R}^{T \times 165}$, $P_{\text{PrimeDepth}} \in \mathbb{R}^{T \times 576}$, $P_{\text{Sapiens}} \in \mathbb{R}^{T \times 576}$. The dimensionality of each pose type reflects its specific information structure. For instance, DWPose contains 18 body keypoints, 21 keypoints for each hand, and 68 facial keypoints, along with their respective confidence scores, totaling 384 dimensions per frame.

As shown in Fig. 2, we flatten the information from each frame into a 1-dimensional list, concatenate five types of poses to form an input of length 1959, which is then passed through projection layers for simple transformation and dimension matching; this is then followed by the fusion layer for multimodal integration. In this way, we obtain rich pose information for each frame. This standardized structure not only prevents different types of pose information from interfering with each other, but also makes heterogeneous types of pose information mutually compatible.

3.2 Step I: ViT for Multimodal Pose Fusion

In order to ensure that the multi-track pose features are meaningful, we first conduct a simple training to enable the fused posture features to be easily converted into text: We modified the pose entry to output layer of ViT approach that learns the mapping from the unified pose representation to natural language descriptions. It consists of several key components: a pose encoder for multimodal fusion, some layers for the feature processing, and a text decoder for generating the final output.

We choose ViT for pose latent space construction because: (1) ViT’s self-attention mechanism can effectively fuse heterogeneous pose representations from different extraction tools (SMPLer-X, DWPose, Mediapipe, PrimeDepth, Sapiens) into a unified latent space. (2) ViT’s deep layered architecture naturally creates a hierarchical latent space that can compress rich, multi-source pose in-

formation into compact representations while preserving essential pose details—making it an ideal container for our pose-rich latent space. (3) Unlike specialized VAE encoders (He et al., 2022), ViT’s transformer architecture can scale well to high-dimensional inputs, enabling us to replicate Stable Diffusion’s success of operating in compact latent space for the sign language domain.

Multimodal Pose Fusion Layer. The pose encoder E_{pose} processes the five types of pose information with type-specific encoders and fuses them through a multi-head attention mechanism:

$$\begin{aligned} f_i &= E_i(P_i), \\ f_{\text{fused}} &= \text{MultiHeadAttention}(f_1, f_2, \dots, f_5) \end{aligned} \quad (1)$$

where E_i is the encoder for pose type i , and $f_i \in \mathbb{R}^{d_h}$ is the encoded feature. This fusion approach preserves the unique characteristics of each pose type, while allowing information sharing among them (Ko et al., 2019b; Liu et al., 2022; Zhang et al., 2020).

For each f_i , we project it to a unified representation space through a dimension matching layer:

$$z_i = \text{PadMatch}(f_i) \in \mathbb{R}^{2048} \quad (2)$$

where z_i is the unified representation at position i ; PadMatch refers to zero-padding followed by projection. The ViT layers process this unified representation through multi-head self-attention and cross-attention mechanisms:

$$z_{\text{latent}} = \text{ViT}_{\text{layers}}(z_1, z_2, \dots, z_n) \quad (3)$$

where z_{latent} represents the final pose-rich latent representation that captures the essence of sign language movements (Stoll et al., 2020; Cho et al., 2021; Lu et al., 2023a).

Custom CodeBook Decoder. We initially attempted to use T5 (Raffel et al., 2020), currently one of the most popular text decoders, as our text decoding component. However, experimental results revealed that for sign language translation tasks, we only need to consider the vocabulary present in our specific dataset. Large-scale decoders like T5 not only reduce inference speed, but also increase error probability, potentially generating words that do not exist in our target vocabulary $\mathcal{V}_{\text{dataset}}$. Therefore, we developed a custom CodeBook using training data, where the model outputs vocabulary indices rather than raw text tokens, significantly improving accuracy.

3.3 Step II: ViT for Video2Pose

To process raw video inputs directly, we develop a Video2Pose module based on video entry of ViT (Dosovitskiy et al., 2021). Given an input video $V \in \mathbb{R}^{T \times H \times W \times 3}$, the Video2Pose module extracts frame-level features and models their temporal relationships:

$$V_{\text{frame}} = v_1, v_2, \dots, v_T = \text{ViT}_{\text{spatial}}(V) \quad (4)$$

where $v_t \in \mathbb{R}^{d_v}$ represents the feature of frame t extracted by the spatial ViT. To capture temporal dependencies, we employ a temporal attention mechanism:

$$V_{\text{temp}} = \text{TemporalAttention}(V_{\text{frame}}) \quad (5)$$

The Video2Pose module then projects these temporal features to the same format as the five pose types:

$$\hat{P}_i = \text{Projection}_i(V_{\text{temp}}) \quad (6)$$

where \hat{P}_i is the predicted pose of type i . This end-to-end approach eliminates the need for separate pose extraction models during deployment, greatly simplifying the application process (Saunders et al., 2021b; Tarrés et al., 2023; Chen et al., 2020; Xie et al., 2021, 2022).

4 Continuous Sign Language Recognition in the Latent Space

In the previous section, we described construction of a latent space based on ViT and through simple training, it was able to convert the original video into meaningful representations. Next, we should develop an identification method that is trained in the latent space.

4.1 Latent Feature Organization and Optimization

Pose-Aware Feature Compilation. Before the temporal learner can reason over sequences, we enforce a disciplined organization of the features produced by the Vid2Pose encoder. Every frame-level embedding $z_t \in \mathbb{R}^{2048}$ is accompanied by its gloss supervision signal g_t and confidence mask m_t , giving us a richer tuple $\langle z_t, g_t, m_t \rangle$. As shown in Fig. 3, this tuple is passed through a *lightweight transformer stack* that performs (i) variance-preserving layer normalization, (ii) cross-frame covariance whitening (using coefficient γ), and (iii) stochastic frame dropping (with probability ρ) to avoid overfitting to repetitive segments. The process aligns

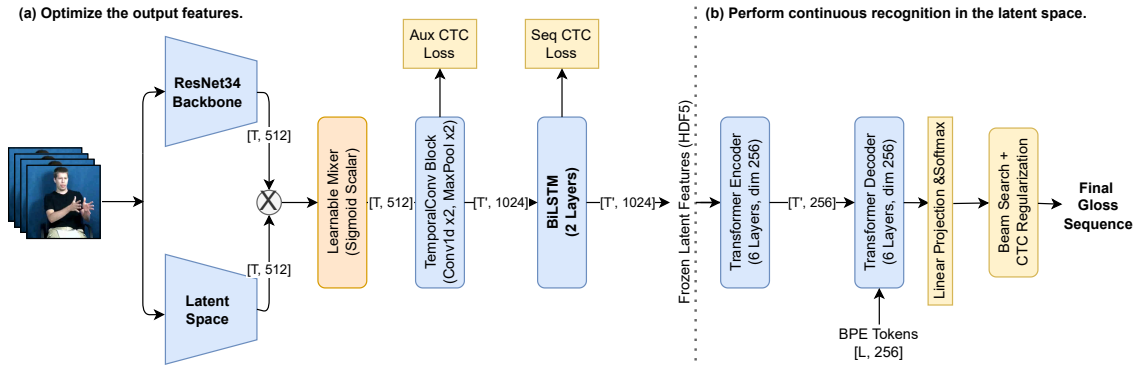


Figure 3: **Organize and conduct continuous recognition in the latent space:** (a) For the latent space of the enriched poses, we further distill, compress and organize it. The number of features trained should be as aligned as possible with the number of Gloss. This can further enhance the upper limit and performance of our model. (b) Then, we develop it based on a BiLSTM method (Zhang et al., 2023a), enabling it to perform continuous Sign recognition in this latent space, thereby achieving results far superior to previous works.

Algorithm 1 PoseAwareFeatureCompilation

```

1: procedure COMPILER( $\{z_t, g_t, m_t\}_{t=1}^T$ )
2:    $z_t \leftarrow \text{LayerNorm}(z_t)$ 
3:    $c_t \leftarrow \text{CrossCov}(z_t, z_{t-1})$ 
4:    $z_t \leftarrow z_t - \gamma \cdot c_t$   $\triangleright$  Covariance whitening
5:   if Bernoulli( $\rho$ ) = 1 then
6:      $z_t \leftarrow \mathbf{0}; m_t \leftarrow 0$   $\triangleright$  Stochastic frame drop
7:   end if
8:    $a_t \leftarrow \text{GlossAlign}(z_t, g_t)$ 
9:   return  $\{(z_t, a_t, m_t)\}_{t=1}^T$ 
10: end procedure

```

pose cues with textual semantics via a *GlossAlign* function this process is formalized in Algorithm 1. Here, *GlossAlign* assigns each feature to its corresponding gloss based on temporal overlap, and *CrossCov* (Zhang et al., 2023a) computes the cross-covariance between consecutive frames for redundancy detection.

Gloss-Aware Latent Distillation. With the compiled tuples we run a *knowledge distillation* objective that pushes the latent vectors toward a compact space guided by gloss embeddings. A teacher backbone f_{ResNet} (based on ResNet-34) produces logits y_t^{teacher} , while the latent vectors generate student logits y_t^{student} through a two-layer perceptron. The KL divergence between both streams, weighted by gloss frequency priors, ensures that rare glosses receive more attention. This mirrors the *SeqKD* objective but operates entirely within our latent pose space. Algorithm 2 presents the complete hierarchical training procedure.

Adaptive Feature Pruning. To optimize the information density of the latent space, we monitor each latent dimension’s importance during training using its *Fisher information*. Specifically, dimensions whose activation variance fails to surpass a dynamic threshold τ are identified as redundant and subsequently pruned:

$$\text{Prune } z^{(d)} \text{ if } \text{Var}(z^{(d)}) < \tau \quad (7)$$

This mechanism reduces the effective latent width to approximately 1024, which forces the model to grasp the similarities and differences between different pose formats. To ensure structural compatibility with the subsequent BiLSTM and Transformer layers without altering tensor shapes, we implement this as a masking operation:

$$\hat{z}_t = z_t \odot M, \quad M_d = \begin{cases} 1 & \text{if } \text{Var}(z^{(d)}) \geq \tau \\ 0 & \text{otherwise} \end{cases} \quad (8)$$

This pruning step is triggered every K iterations and is synchronized with the checkpoint averaging routine to maintain stability during the transition.

Multi-Scale Feature Augmentation. To combat data scarcity in sign language datasets, we apply a $N = 10$ -fold temporal augmentation during feature extraction (Zhang et al., 2023a). For each video sample i , the SMKD model (Zhang et al., 2023a) generates N augmented versions through (i) random temporal scaling $\sigma \in [0.8, 1.2]$, (ii) spatial jittering with probability $p_{jit} = 0.3$, and (iii) feature-space Gaussian noise $\mathcal{N}(0, 0.01)$. The augmented features are stored in HDF5 format with keys $\{i\}_j$ where $j \in [0, N-1]$ indexes the augmentation version. It enables efficient random access

Algorithm 2 HierarchicalLatentTraining

```

1: procedure TRAINLATENT( $\mathcal{D}$ )
2:   for epoch = 1 . . .  $E$  do
3:     for batch  $\in \mathcal{D}$  do
4:        $\{(z_t, a_t, m_t)\}$   $\leftarrow$ 
         COMPILER(batch)
5:        $y^{\text{teacher}} \leftarrow f_{\text{ResNet}}(\text{batch})$ 
6:        $y^{\text{student}} \leftarrow f_{\text{MLP}}(\{z_t\})$ 
7:        $\mathcal{L}_{\text{KD}} \leftarrow \text{KL}(y^{\text{student}}, y^{\text{teacher}})$ 
8:        $\mathcal{L}_{\text{CTC}}$   $\leftarrow$ 
         CTC( $y^{\text{student}}$ , gloss labels)
9:        $\mathcal{L} \leftarrow \lambda_{\text{KD}}\mathcal{L}_{\text{KD}} + \lambda_{\text{CTC}}\mathcal{L}_{\text{CTC}}$ 
10:      Update parameters via Adam
11:    end for
12:    if epoch mod  $K = 0$  then
13:      Prune dims with  $\text{Var}(z^{(d)}) < \tau$ 
14:    end if
15:  end for
16: end procedure

```

during training while expanding the effective data size from M to $M \times N$ samples. Unlike pixel-space augmentation which requires re-encoding, our latent augmentation operates on extracted features, reducing computational overhead.

4.2 Latent-Space Temporal Modeling and Decoding

Hybrid Temporal Modeling. The distilled latent sequences feed a hybrid backbone that remains modality-agnostic. First, a *TemporalConv stack* (two K5 blocks interleaved with stride-2 pooling) compresses sequences from T frames to $T' \approx T/4$, producing features $h_t \in \mathbb{R}^{1024}$. These features then pass through a *bidirectional LSTM* (2 layers, hidden size 512 per direction) to capture long-range dependencies, yielding $u_t \in \mathbb{R}^{1024}$. Because all computations remain within the latent space, we avoid heavy pixel-level operations during inference.

CTC-Constrained Transformer Refinement. A *Transformer encoder-decoder* (6 layers each, width 256) refines the BiLSTM outputs into gloss sequences. The encoder ingests u_t after projection to 256 dimensions, whereas the decoder consumes BPE-tokenized gloss strings. We attach a *CTC head* directly to the encoder outputs to enforce monotonic alignment, ensuring the architecture accepts the latent tensors without additional reshaping. The joint objective combines sequence-level cross-entropy, encoder-side CTC, and a *latent-*

Algorithm 3 LatentSequenceDecoding

```

1: procedure DECODE( $H = \{u_t\}_{t=1}^{T'}$ , beam size  $B$ )
2:   Initialize beams  $\mathcal{B} \leftarrow \{\langle \text{BOS}, 0 \rangle\}$ 
3:   for  $t = 1 \dots T_{\text{max}}$  do
4:      $\mathcal{B}' \leftarrow \emptyset$ 
5:     for hypothesis  $\langle y, s \rangle \in \mathcal{B}$  do
6:        $p(\cdot) \leftarrow \text{DecoderStep}(y, H)$ 
7:       for token  $w$  in top- $k$  of  $p$  do
8:          $s' \leftarrow s + \log p(w) - \alpha \cdot$ 
           AttnEntropy( $y, H$ )
9:          $\mathcal{B}' \leftarrow \mathcal{B}' \cup \{\langle y \oplus w, s' \rangle\}$ 
10:      end for
11:    end for
12:     $\mathcal{B} \leftarrow$  top- $B$  of  $\mathcal{B}'$ 
13:    if all beams end with EOS then break
14:    end if
15:  end for
16:  return best hypothesis in  $\mathcal{B}$ 
17: end procedure

```

space regularizer that encourages successive encoder states to remain within a Lipschitz ball.

Beam Search with Latent Feedback. During inference we run an 8-beam search where each hypothesis carries an auxiliary latent score derived from the *encoder attention entropy*. Hypotheses with erratic attention (high entropy) incur a penalty α , biasing the search toward sequences that remain faithful to the latent pose evidence. The final gloss output can therefore be obtained without re-running pose estimators. Algorithm 3 details the complete beam search decoding procedure.

Training Optimization and Regularization. To stabilize convergence and improve generalization, we employ a suite of optimization techniques. The learning rate follows a Noam scheduler (Vaswani et al., 2017) with warmup steps $W = 4000$:

$$\eta(t) = d_{\text{model}}^{-0.5} \cdot \min(t^{-0.5}, t \cdot W^{-1.5}) \quad (9)$$

where $d_{\text{model}} = 256$. We apply *differentiated dropout* with rates tailored to each component: $p_{\text{attn}} = 0.3$ for attention weights, $p_{\text{relu}} = 0.5$ for activation layers, and $p_{\text{res}} = 0.4$ for residual connections, preventing over-reliance on any single pathway. Label smoothing with $\epsilon = 0.1$ regularizes the output distribution. Finally, we adopt *checkpoint averaging* over the top-5 models ranked by validation WER.

ASLLRP											
Method	Dev					Test					
	Rouge	BLEU1	BLEU2	BLEU3	BLEU4	Rouge	BLEU1	BLEU2	BLEU3	BLEU4	
Sign2Gloss	C2SLR (Zuo and Mak, 2022)	52.50	50.10	38.20	29.50	24.76	52.30	49.95	38.00	29.35	24.58
	CorrNet+ (Hu et al., 2024)	53.80	51.40	39.50	31.20	26.14	53.60	51.25	39.30	31.05	25.96
	SLTUNET (Zhang et al., 2023a)	54.20	52.10	40.10	31.80	26.48	54.05	51.90	39.95	31.65	26.31
	SignX (Ours)	56.65	51.84	42.48	35.35	29.80	56.48	51.65	42.31	35.19	29.64

Table 1: **Benchmark on the ASLLRP dataset** (Neidle et al., 2022a; Neidle and Metaxas, 2025). To ensure a fair and rigorous comparison on the ASLLRP dataset, we re-implemented and fine-tuned several representative SLR frameworks, including C2SLR and SLTUNET, achieving their best possible performance as modern baselines.

SignX (Ours)
<p><i>Generated Text:</i> IF STUDENT IX HEAR/LISTEN TEACH+AGENT FUTURE LEARN SOMETHING/ONE</p> <p><i>Ground Truth:</i> IF STUDENT IX HEAR/LISTEN TEACH+AGENT FUTURE LEARN SOMETHING/ONE</p>
<p><i>Generated Text:</i> BOX/ROOM IX NOT-YET ARRIVE IX SHOULD CONTACT ns-fs-FEDEX</p> <p><i>Ground Truth:</i> BOX/ROOM IX NOT-YET ARRIVE IX SHOULD CONTACT ns-fs-FEDEX</p>
<p><i>Generated Text:</i> PEOPLE ARRIVE LATE WHO</p> <p><i>Ground Truth:</i> PERSON ARRIVE LATE WHO</p>
<p><i>Generated Text:</i> HERE ns-fs-MARY FUTURE PAY/BUY CAR</p> <p><i>Ground Truth:</i> MAYBE ns-fs-MARY FUTURE PAY/BUY CAR</p>

Table 2: **Qualitative evaluation of translation results on the ASLLRP dataset.** The examples demonstrate successful reconstructions of long-form gloss sequences and specialized fingerspelling, as well as minor failure cases. Other examples can be found in Section D.4.

5 Experimental Results

Here, we evaluate our SignX continuous recognition method on mainstream datasets (ASLLRP (Neidle and Metaxas, 2025): 2,669 utterances; PHOENIX2014-T (Camgöz et al., 2018): 7,096/519/642 train/val/test; CSL-Daily (Zhou et al., 2021b): 18,401/1,077/1,176; WLASL-2000 (Li et al., 2020a): 2,000 signs), using metrics such as Bleu (Papineni et al., 2002), WER (Klakow and Peters, 2002), and P-I (Li et al., 2020b). We conduct a series of experiments including qualitative, quantitative, ablation, and efficiency evaluations, demonstrating that our method has achieved a significant improvement over the state-of-the-art².

5.1 Qualitative Assessment

SignX consistently reproduces sentence-level semantics on long-form conditionals (Table 2, first row), suggesting that the hierarchical design effectively preserves subject–temporal relations over extended contexts. The second sample highlights a specialized strength in accurately capturing fingerspelled entities like “fs-FEDEX” within domain-specific logistics, maintaining the structural fram-

²More mertric information in Section D.1.

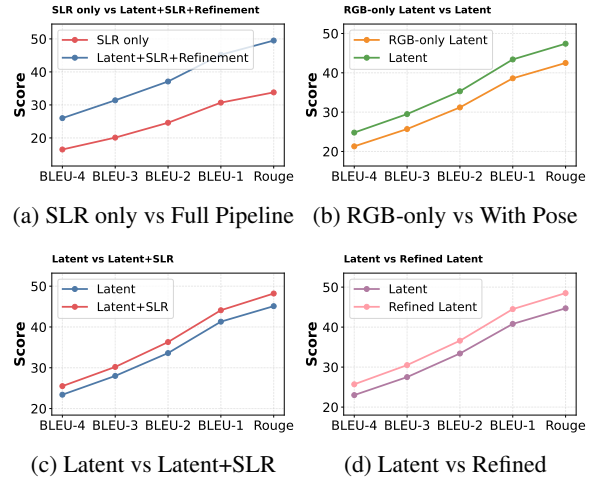


Figure 4: **Ablation Study Results.** Performance comparison across different 1k step model configurations on ASLLRP dev set. (a) Impact of full pipeline components. (b) Effect of pose feature integration. (c) Contribution of sign language recognition module. (d) Improvement from latent refinement. All metrics show that all the changes were necessary and effective. More results are available at Sec. D.2 and Sec. D.3.

ing and lexical integrity entirely intact. The third sample demonstrates the model’s capacity for semantic alignment; although the lexical choice of “PEOPLE” diverges from the ground-truth “PERSON,” the core agentive meaning is successfully recovered through latent synonym mapping. The final example exhibits a minor stylistic drift where the modal adverb “MAYBE” is substituted with “HERE”—a frequent spatial filler in sign language—reflecting a slight divergence in functional modifiers rather than a structural collapse. Overall, the model captures core semantic intent with high fidelity but may substitute ground-truth glosses with semantically refined or nuanced alternatives.

5.2 Quantitative Assessment

5.2.1 Ablation Results

As illustrated in Fig. 4, ablation studies on ASLLRP confirm that our full pipeline significantly outperforms the SLR-only baseline. Specifically,

PHOENIX2014-T											
Method	Dev					Test					
	Rouge	BLEU1	BLEU2	BLEU3	BLEU4	Rouge	BLEU1	BLEU2	BLEU3	BLEU4	
Sign2Text	SL-Luong (Camgöz et al., 2018)	31.80	31.87	19.11	13.16	9.94	31.80	32.24	19.03	12.83	9.58
	Joint-SLRT (Cihan Camgöz et al., 2020)	-	47.26	34.40	27.05	22.38	-	46.61	33.73	26.19	21.32
	STMC-T (Zhou et al., 2021c)	48.24	47.60	36.43	29.18	24.09	46.65	46.98	36.09	28.70	23.65
	SignBT (Zhou et al., 2021b)	50.29	51.11	37.90	29.80	24.45	49.54	50.80	37.75	29.72	24.32
	MMTLB (Chen et al., 2022a)	53.10	53.95	41.12	33.14	27.61	52.65	53.97	41.75	33.84	28.39
	SLTUNET (Zhang et al., 2023a)	52.23	-	-	-	27.87	52.11	52.92	41.76	33.99	28.47
	TwoStream-SLT (Chen et al., 2022b)	54.08	54.32	41.99	34.15	28.66	53.48	54.90	42.43	34.46	28.95
	CorrNet+ (Hu et al., 2024)	54.54	54.56	42.31	34.48	29.13	53.76	55.32	42.74	34.86	29.42
	SignX (Ours)	55.32	55.24	43.10	35.45	30.08	55.15	55.08	42.92	35.28	29.91
CSL-Daily											
Method	Dev					Test					
	Rouge	BLEU1	BLEU2	BLEU3	BLEU4	Rouge	BLEU1	BLEU2	BLEU3	BLEU4	
Sign2Text	SL-Luong (Camgöz et al., 2018)	34.28	34.22	19.72	12.24	7.96	34.54	34.16	19.57	11.84	7.56
	SignBT (Zhou et al., 2021b)	49.49	51.46	37.23	27.51	20.80	49.31	51.42	37.26	27.76	21.34
	MMTLB (Chen et al., 2022a)	53.38	53.81	40.84	31.29	24.42	53.25	53.31	40.41	30.87	23.92
	SLTUNET (Zhang et al., 2023a)	53.58	-	-	-	23.99	54.08	54.98	41.44	31.84	25.01
	TwoStream-SLT (Chen et al., 2022b)	55.10	55.21	42.31	32.71	25.76	55.72	55.44	42.59	32.87	25.79
	CorrNet+ (Hu et al., 2024)	55.52	55.64	42.78	33.13	26.14	55.84	55.82	42.96	33.26	26.14
	Uni-Sign (Li et al., 2025)	56.03	55.30	-	-	26.25	56.51	55.08	-	-	26.36
	SignX (Ours)	57.25	57.10	44.50	35.80	28.75	57.12	56.95	44.32	35.62	28.58

Table 3: **Comparison with state-of-the-art methods** on the PHOENIX2014-T dataset (Camgöz et al., 2018) and CSL-Daily dataset (Zhou et al., 2021b) over the SLT setting. “-”: Information is unavailable.

Method	Continuous SLR (CSLR)		Isolated SLR (ISLR)	
	RWTH-14T (WER ↓)	CSL-Daily (WER ↓)	Method	WLASL-2000 (P-I ↑)
GEU (Tang et al., 2022)	49.9	-	SignBERT (Hu et al., 2021)	39.40
SLT (Cihan Camgöz et al., 2020)	24.5	32.0	BEST (Zhao et al., 2023)	46.25
Bert (Guo et al., 2024)	21.2	30.8	SignBERT+ (Hu et al., 2023a)	48.85
Bert fine-tuning (Guo et al., 2024)	20.4	30.0	MSLU (Zhou et al., 2025)	56.29
CorrNet (Hu et al., 2023b)	20.5	30.1	NLA-SLR (Zuo et al., 2023)	61.05
GPGN (Guo et al., 2024)	20.5	30.0	Uni-Sign (Li et al., 2025)	63.52
CorrNet+ (Hu et al., 2024)	19.1	28.2	Sigma (Pu et al., 2025)	64.40
SignX (Ours)	18.6	24.3	SignX (Ours)	68.29

Table 4: **Comprehensive Comparison on Continuous and Isolated SLR.** Left: WER on RWTH-2014-T and CSL-Daily. Right: P-I accuracy on WLASL-2000. Our SignX framework achieves SOTA performance across all tracks, even when compared with the latest Sigma (Pu et al., 2025) from the same period.

pose features provide critical spatial cues, while the SLR module and latent refinement mechanism enhance intermediate supervision and temporal coherence, validating each component’s necessity in capturing complex sign language semantics. All experiments exhibit consistent improvement trends across metrics, collectively validating each component’s necessity in our framework.

5.3 Comparison with Previous Work

We evaluate the **SignX** framework across multiple mainstream benchmarks (Camgoz et al., 2018b; Zhou et al., 2021a; Li et al., 2020b), utilizing a comprehensive suite of metrics including WER, BLEU, and P-I accuracy. As illustrated in tables 3 and 4, SignX achieves significant improvements over current state-of-the-art methods in both continuous sign recognition and isolated sign recognition tasks (Note that some of the SLT work is different from

ours and cannot be directly compared, e.g., (Zhang et al., 2025)), our framework establishes a new performance ceiling, exhibiting superior robustness and cross-domain scalability, thereby providing a high-performance baseline for CSLR task.

6 Conclusion

This paper presents **SignX**, a high-efficiency framework for CSLR. (i) By leveraging Vision Transformers (ViT) (Dosovitskiy et al., 2021), we construct a unified and information-dense latent space that successfully integrates heterogeneous pose representations from five state-of-the-art estimators. (ii) This latent space is further refined through multi-faceted techniques for compression, structural organization, and semantic alignment, establishing a robust sign-specific representation space that effectively maps raw sign language videos to latent embeddings. (iii) Furthermore, we perform continuous recognition within this compressed, pose-rich space by employing a multi-stage modeling approach that combines ResNet-driven (Zhang et al., 2023a) temporal feature distillation with Transformer-based sequence refinement, supplemented by latent optimization strategies such as covariance whitening and adaptive pruning. (iv) **SignX** significantly enhances recognition accuracy while drastically reducing computational overhead. Extensive experimental validation across four major benchmarks —demonstrates that **SignX** achieves SOTA performance across all metrics.

Limitations

SignX achieves a significant performance ceiling by adopting a **structured, modular training paradigm**. While this approach involves a sequence of specialized optimization steps compared to monolithic end-to-end models, this design choice is a **deliberate and beneficial trade-off**. Drawing an analogy to **Latent Diffusion Models**, components like the VAE and UNet can be decoupled or substituted; although they constitute a single system, the modules remain functionally separable. This modularity is a primary driver of their popularity, as it significantly **alleviates the computational and training burden**. Our architecture follows the same principle, ensuring that the **overall net gain** in efficiency and stability outweighs the orchestration complexity.

References

- Matyáš Boháček and Marek Hruš. Sign pose-based transformer for word-level sign language recognition. In *Proceedings of the IEEE/CVF Winter Conference on Applications of Computer Vision (WACV) Workshops*, pages 182–191, 2022.
- Zhongang Cai, Wanqi Yin, Ailing Zeng, Chen Wei, Qingping Sun, Yanjun Wang, Hui En Pang, Haiyi Mei, Mingyuan Zhang, Lei Zhang, Chen Change Loy, Lei Yang, and Ziwei Liu. Smpler-x: Scaling up expressive human pose and shape estimation, 2023.
- Necati Cihan Camgoz, Simon Hadfield, Oscar Koller, Hermann Ney, and Richard Bowden. Neural sign language translation. In *2018 IEEE/CVF Conference on Computer Vision and Pattern Recognition*, pages 7784–7793, 2018a.
- Necati Cihan Camgoz, Simon Hadfield, Oscar Koller, Hermann Ney, and Richard Bowden. Neural sign language translation. In *2018 IEEE/CVF Conference on Computer Vision and Pattern Recognition*, pages 7784–7793, 2018b.
- Necati Cihan Camgöz, Simon Hadfield, Oscar Koller, Hermann Ney, and Richard Bowden. Neural Sign Language Translation. In *Proceedings of the IEEE Conference on Computer Vision and Pattern Recognition (CVPR)*, 2018.
- Zhe Cao, Gines Hidalgo, Tomas Simon, Shih-En Wei, and Yaser Sheikh. OpenPose: Realtime Multi-Person 2D Pose Estimation using Part Affinity Fields. In *Proceedings of the IEEE Conference on Computer Vision and Pattern Recognition (CVPR)*, 2017.
- J. Carreira and A. Zisserman. Quo vadis, action recognition? a new model and the kinetics dataset. In *Proceedings of the IEEE/CVF Conference on Computer Vision and Pattern Recognition (CVPR)*, 2017.
- Caroline Chan, Shiry Ginosar, Tinghui Zhou, and Alexei A Efros. Everybody Dance Now. In *Proceedings of the IEEE International Conference on Computer Vision (CVPR)*, 2019.
- James Charles, Tomas Pfister, Mark Everingham, and Andrew Zisserman. Automatic and Efficient Human Pose Estimation for Sign Language Videos. *International Journal of Computer Vision (IJCV)*, 2014.
- Ting Chen, Simon Kornblith, Mohammad Norouzi, and Geoffrey Hinton. A simple framework for contrastive learning of visual representations. *arXiv preprint arXiv:2002.05709*, 2020.
- Xuanting Chen, Junjie Ye, Can Zu, Nuo Xu, Rui Zheng, Minglong Peng, Jie Zhou, Tao Gui, Qi Zhang, and Xuanjing Huang. How robust is gpt-3.5 to predecessors? a comprehensive study on language understanding tasks, 2023.
- Yutong Chen, Fangyun Wei, Xiao Sun, Zhirong Wu, and Stephen Lin. A simple multi-modality transfer learning baseline for sign language translation. In *Proceedings of the IEEE/CVF Conference on Computer Vision and Pattern Recognition*, pages 5120–5130, 2022a.
- Yutong Chen, Ronglai Zuo, Fangyun Wei, Yu Wu, Shujie Liu, and Brian Mak. Two-stream network for sign language recognition and translation. *NeurIPS*, 2022b.
- Hung-Yueh Chiang, Yen-Liang Lin, Yueh-Cheng Liu, and Winston H Hsu. A unified point-based framework for 3d segmentation. In *3DV*, 2019.
- Jaemin Cho, Jie Lei, Hao Tan, and Mohit Bansal. Unifying vision-and-language tasks via text generation. In *International Conference on Machine Learning*, pages 1931–1942. PMLR, 2021.
- Necati Cihan Camgoz, Simon Hadfield, Oscar Koller, Hermann Ney, and Richard Bowden. Neural sign language translation. In *CVPR*, pages 7784–7793, 2018.
- Necati Cihan Camgöz, Oscar Koller, Simon Hadfield, and Richard Bowden. Sign Language Transformers: Joint End-to-end Sign Language Recognition and Translation. In *Proceedings of the IEEE Conference on Computer Vision and Pattern Recognition (CVPR)*, 2020.
- Necati Cihan Camgöz, Oscar Koller, Simon Hadfield, and Richard Bowden. Sign language transformers: Joint end-to-end sign language recognition and translation. In *2020 IEEE/CVF Conference on Computer Vision and Pattern Recognition (CVPR)*, 2020.
- Helen Cooper and Richard Bowden. Large Lexicon Detection of Sign Language. In *International Workshop on Human-Computer Interaction*, 2007.
- Runpeng Cui, Hu Liu, and Changshui Zhang. Recurrent Convolutional Neural Networks for Continuous Sign Language Recognition by Staged Optimization. In *Proceedings of the IEEE Conference on Computer Vision and Pattern Recognition (CVPR)*, 2017.
- Runpei Dong, Zekun Qi, Linfeng Zhang, Junbo Zhang, Jianjian Sun, Zheng Ge, Li Yi, and Kaisheng Ma. Autoencoders as cross-modal teachers: Can pretrained 2d image transformers help 3d representation learning? *arXiv preprint arXiv:2212.08320*, 2022.
- Alexey Dosovitskiy, Lucas Beyer, Alexander Kolesnikov, Dirk Weissenborn, Xiaohua Zhai, Thomas Unterthiner, Mostafa Dehghani, Matthias Minderer, Georg Heigold, Sylvain Gelly, Jakob Uszkoreit, and Neil Houlsby. An image is worth 16x16 words: Transformers for image recognition at scale. *ICLR*, 2021.

- Amanda Duarte, Shruti Palaskar, Lucas Ventura, Deepti Ghadiyaram, Kenneth DeHaan, Florian Metze, Jordi Torres, and Xavier Giro-i Nieto. How2Sign: A Large-scale Multimodal Dataset for Continuous American Sign Language. In *Proceedings of the IEEE/CVF Conference on Computer Vision and Pattern Recognition (CVPR)*, 2021a.
- Amanda Duarte, Shruti Palaskar, Lucas Ventura, Deepti Ghadiyaram, Kenneth DeHaan, Florian Metze, Jordi Torres, and Xavier Giro-i Nieto. How2Sign: A Large-Scale Multimodal Dataset for Continuous American Sign Language. In *Proceedings of the IEEE/CVF Conference on Computer Vision and Pattern Recognition (CVPR)*, 2021b.
- Sen Fang, Chen Chen, Lei Wang, Ce Zheng, Chunyu Sui, and Yapeng Tian. Signllm: Sign language production large language models, 2025a.
- Sen Fang, Yalin Feng, Hongbin Zhong, Yanxin Zhang, and Dimitris N. Metaxas. Stable signer: Hierarchical sign language generative model, 2025b.
- Sen Fang, Chunyu Sui, Yanghao Zhou, Xuedong Zhang, Hongbin Zhong, Yapeng Tian, and Chen Chen. Signdiff: Diffusion model for american sign language production, 2025c.
- Sen Fang, Hongbin Zhong, Yalin Feng, and Dimitris N. Metaxas. Streamflow: Theory, algorithm, and implementation for high-efficiency rectified flow generation, 2025d.
- Jens Forster, Christoph Schmidt, Thomas Hoyoux, Oscar Koller, Uwe Zelle, Justus H Piater, and Hermann Ney. RWTH-PHOENIX-Weather: A Large Vocabulary Sign Language Recognition and Translation Corpus. In *Proceedings of the International Conference on Language Resources and Evaluation (LREC)*, 2012.
- Kirsti Grobel and Marcell Assan. Isolated Sign Language Recognition using Hidden Markov Models. In *IEEE International Conference on Systems, Man, and Cybernetics*, 1997.
- Rıza Alp Güler, Natalia Neverova, and Iasonas Kokkinos. Densepose: Dense human pose estimation in the wild. In *Proceedings of the IEEE Conference on Computer Vision and Pattern Recognition*, pages 7297–7306, 2018.
- Leming Guo, Wanli Xue, Bo Liu, Kaihua Zhang, Tiantian Yuan, and Dimitris Metaxas. Gloss prior guided visual feature learning for continuous sign language recognition. *IEEE Transactions on Image Processing*, 33:3486–3495, 2024.
- Kaiming He, Xiangyu Zhang, Shaoqing Ren, and Jian Sun. Deep residual learning for image recognition. In *2016 IEEE Conference on Computer Vision and Pattern Recognition (CVPR)*, pages 770–778, 2016.
- Kaiming He, Xinlei Chen, Saining Xie, Yanghao Li, Piotr Dollár, and Ross Girshick. Masked autoencoders are scalable vision learners. In *Proceedings of the IEEE/CVF Conference on Computer Vision and Pattern Recognition*, pages 16000–16009, 2022.
- Shawn Hershey, Sourish Chaudhuri, Daniel PW Ellis, Jort F Gemmeke, Aren Jansen, R Channing Moore, Manoj Plakal, Devin Platt, Rif A Saurous, Bryan Seybold, et al. Cnn architectures for large-scale audio classification. In *2017 IEEE International Conference on Acoustics, Speech and Signal Processing (ICASSP)*, pages 131–135. IEEE, 2017.
- Jonathan Ho, Ajay Jain, and Pieter Abbeel. Denoising diffusion probabilistic models. *arXiv preprint arxiv:2006.11239*, 2020.
- Hezhen Hu, Weichao Zhao, Wengang Zhou, Yuechen Wang, and Houqiang Li. Signbert: Pre-training of hand-model-aware representation for sign language recognition. In *Proceedings of the IEEE/CVF international conference on computer vision*, pages 11087–11096, 2021.
- Hezhen Hu, Weichao Zhao, Wengang Zhou, and Houqiang Li. Signbert+: Hand-model-aware self-supervised pre-training for sign language understanding. *IEEE Transactions on Pattern Analysis and Machine Intelligence*, 45(9):11221–11239, 2023a.
- Lianyu Hu, Liqing Gao, Zekang Liu, and Wei Feng. Continuous sign language recognition with correlation network. In *Proceedings of the IEEE/CVF International Conference on Computer Vision*, 2023b.
- Lianyu Hu, Wei Feng, Liqing Gao, Zekang Liu, and Liang Wan. Cornnet+: Sign language recognition and translation via spatial-temporal correlation, 2024.
- Wencan Huang, Wenwen Pan, Zhou Zhao, and Qi Tian. Towards Fast and High-Quality Sign Language Production. In *Proceedings of the 29th ACM International Conference on Multimedia*, 2021.
- Timor Kadir, Richard Bowden, Eng-Jon Ong, and Andrew Zisserman. Minimal Training, Large Lexicon, Unconstrained Sign Language Recognition. In *Proceedings of the British Machine Vision Conference (BMVC)*, 2004.
- Slava M. Katz. Estimation of probabilities from sparse data for the language model component of a speech recognizer. *IEEE Trans. Acoust. Speech Signal Process.*, 35(3):400–401, 1987.
- Rawal Khirodkar, Timur Bagautdinov, Julieta Martinez, Su Zhaoen, Austin James, Peter Selednik, Stuart Anderson, and Shunsuke Saito. Sapiens: Foundation for human vision models. *arXiv preprint arXiv:2408.12569*, 2024.
- Youngmin Kim, Minji Kwak, Dain Lee, Yeongeun Kim, and Hyeonbo Baek. Keypoint based sign language translation without glosses. *arXiv preprint arXiv:2204.10511*, 2022.
- Diederik P Kingma and Max Welling. Auto-encoding variational bayes. *arXiv preprint arXiv:1312.6114*, 2013.
- Dietrich Klakow and Jochen Peters. Testing the correlation of word error rate and perplexity. *Speech Communication*, 38(1):19–28, 2002.
- Sang-Ki Ko, Chang Jo Kim, Hyedong Jung, and Choongsang Cho. Neural sign language translation based on human keypoint estimation. *Applied sciences*, 9(13):2683, 2019a.
- Sang-Ki Ko, Chang Jo Kim, Hyedong Jung, and Choongsang Cho. Neural Sign Language Translation based on Human Keypoint Estimation. *Applied Sciences*, 2019b.
- Oscar Koller. Quantitative Survey of the State of the Art in Sign Language Recognition. *arXiv preprint arXiv:2008.09918*, 2020.

- Oscar Koller, Jens Forster, and Hermann Ney. Continuous sign language recognition: Towards large vocabulary statistical recognition systems handling multiple signers. *Computer Vision and Image Understanding*, 141:108–125, 2015a.
- Oscar Koller, Jens Forster, and Hermann Ney. Continuous Sign Language Recognition: Towards Large Vocabulary Statistical Recognition Systems Handling Multiple Signers. *Computer Vision and Image Understanding (CVIU)*, 2015b.
- Jolanta Lapiak. Gloss: transcription symbols. <https://www.handspeak.com/learn/index.php?id=3>. Accessed: 2019-08-20.
- Colin Lea, René Vidal, Austin Reiter, and Gregory D. Hager. Temporal convolutional networks: A unified approach to action segmentation. In *Computer Vision – ECCV 2016 Workshops*, pages 47–54, Cham, 2016. Springer International Publishing.
- Dongxu Li, Cristian Rodriguez, Xin Yu, and Hongdong Li. Word-level deep sign language recognition from video: A new large-scale dataset and methods comparison. In *Proceedings of the IEEE/CVF winter conference on applications of computer vision*, pages 1459–1469, 2020a.
- Dongxu Li, Cristian Rodriguez, Xin Yu, and Hongdong Li. Word-level deep sign language recognition from video: A new large-scale dataset and methods comparison. In *The IEEE Winter Conference on Applications of Computer Vision*, pages 1459–1469, 2020b.
- Zecheng Li, Wengang Zhou, Weichao Zhao, Kepeng Wu, Hezhen Hu, and Houqiang Li. Uni-sign: Toward unified sign language understanding at scale. *arXiv preprint arXiv:2501.15187*, 2025.
- Scott K Liddell et al. *Grammar, gesture, and meaning in American Sign Language*. Cambridge University Press, 2003.
- Zhijian Liu, Haotian Tang, Alexander Amini, Xinyu Yang, Huiyi Mao, Daniela Rus, and Song Han. Bevfusion: Multi-task multi-sensor fusion with unified bird’s-eye view representation. *arXiv preprint arXiv:2205.13542*, 2022.
- Matthew Loper, Naureen Mahmood, Javier Romero, Gerard Pons-Moll, and Michael J. Black. SMPL: A skinned multi-person linear model. In *ACM TOG*, 2015.
- Jiasen Lu, Christopher Clark, Rowan Zellers, Roozbeh Motlaghi, and Aniruddha Kembhavi. UNIFIED-IO: A Unified Model for Vision, Language, and Multi-modal Tasks. 2023a.
- Yujie Lu, Pan Lu, Zhiyu Chen, Wanrong Zhu, Xin Eric Wang, and William Yang Wang. Multimodal procedural planning via dual text-image prompting. *CoRR*, abs/2305.01795, 2023b.
- Camillo Lugeschi, Jiuqiang Tang, Hadon Nash, Chris McClanahan, Esha Uboweja, Michael Hays, Fan Zhang, Chuoling Chang, Ming Guang Yong, Juhyun Lee, et al. Mediapipe: A framework for building perception pipelines. *arXiv preprint arXiv:1906.08172*, 2019.
- Anqi Mao, Mehryar Mohri, and Yutao Zhong. Cross-entropy loss functions: Theoretical analysis and applications. In *International conference on Machine learning*, pages 23803–23828. PMLR, 2023.
- D. Metaxas. Deformable model and hmm-based tracking, analysis and recognition of gestures and faces. In *Proceedings International Workshop on Recognition, Analysis, and Tracking of Faces and Gestures in Real-Time Systems. In Conjunction with ICCV’99 (Cat. No.PR00378)*, pages 136–140, 1999.
- Amit Moryossef. Complete toolkit for working with poses. <https://github.com/AmitMY/pose-format/>, 2022.
- Amit Moryossef, Ioannis Tsochantaridis, Roei Yosef Aharoni, Sarah Ebling, and Sridhar Narayanan. Real-time sign language detection using human pose estimation. 2020. <https://www.slrtp.com/>.
- Carol Neidle and Carey Ballard. Why alternative gloss labels will increase the value of the wlasl dataset. 2022.
- Carol Neidle and Dimitris Metaxas. American sign language linguistic research project (asllrp) sign bank. <https://dai.cs.rutgers.edu/dai/s/signbank>, 2025. ASLLRP Continuous Signing Corpora, version 3.
- Carol Neidle, Augustine Opoku, Gregory Dimitriadis, and Dimitris Metaxas. NEW Shared & Interconnected ASL Resources: SignStream@ 3 Software; DAI 2 for Web Access to Linguistically Annotated Video Corpora; and a Sign Bank. In *Language Resources and Evaluation. 8th Workshop on the Representation and Processing of Sign Languages: Involving the Language Community. Miyazaki, Japan, 2018-05-12*, pages 147–154.
- Carol Neidle, Augustine Opoku, and Dimitris Metaxas. ASL Video Corpora & Sign Bank: Resources Available through the American Sign Language Linguistic Research Project (ASLLRP), 2022a.
- Carol Neidle, Augustine Opoku, and Dimitris Metaxas. ASL video corpora & sign bank: Resources available through the American sign language linguistic research project (asllrp), 2022b.
- Kishore Papineni, Salim Roukos, Todd Ward, and Wei-Jing Zhu. Bleu: a method for automatic evaluation of machine translation. In *Proceedings of the 40th Annual Meeting of the Association for Computational Linguistics*, pages 311–318, Philadelphia, Pennsylvania, USA, 2002. Association for Computational Linguistics.
- Muxin Pu, Mei Kuan Lim, Chun Yong Chong, and Chen Change Loy. Sigma: Semantically informative pre-training for skeleton-based sign language understanding, 2025.
- Shi Qiu, Saeed Anwar, and Nick Barnes. Dense-resolution network for point cloud classification and segmentation. In *WACV*, pages 3813–3822, 2021.
- Colin Raffel, Noam Shazeer, Adam Roberts, Katherine Lee, Sharan Narang, Michael Matena, Yanqi Zhou, Wei Li, and Peter J. Liu. Exploring the limits of transfer learning with a unified text-to-text transformer. *Journal of Machine Learning Research*, 21(140):1–67, 2020.
- Manny Rayner, Pierrette Bouillon, Sarah Ebling, Johanna Gerlach, Irene Strasly, and Nikos Tsourakis. An open web platform for rule-based speech-to-sign translation. In *54th Annual Meeting of the Association for Computational Linguistics*, pages 162–168, 2016.
- Robin Rombach, Andreas Blattmann, Dominik Lorenz, Patrick Esser, and Björn Ommer. High-resolution image synthesis with latent diffusion models, 2021.

- Ben Saunders, Necati Cihan Camgoz, and Richard Bowden. Everybody sign now: Translating spoken language to photo realistic sign language video. *arXiv preprint arXiv:2011.09846*, 2020a.
- Ben Saunders, Necati Cihan Camgöz, and Richard Bowden. Progressive Transformers for End-to-End Sign Language Production. In *Proceedings of the European Conference on Computer Vision (ECCV)*, 2020b.
- Ben Saunders, Necati Cihan Camgöz, and Richard Bowden. Continuous 3D Multi-Channel Sign Language Production via Progressive Transformers and Mixture Density Networks. *International Journal of Computer Vision (IJCV)*, 2021a.
- Ben Saunders, Necati Cihan Camgöz, and Richard Bowden. Mixed SIGNals: Sign Language Production via a Mixture of Motion Primitives. In *Proceedings of the International Conference on Computer Vision (ICCV)*, 2021b.
- Ben Saunders, Necati Cihan Camgoz, and Richard Bowden. Skeletal Graph Self-Attention: Embedding a Skeleton Inductive Bias into Sign Language Production. *arXiv preprint arXiv:2112.05277*, 2021c.
- Bowen Shi, Diane Brentari, Greg Shakhnarovich, and Karen Livescu. Open-domain sign language translation learned from online video. *Proceedings of the 2022 Conference on Empirical Methods in Natural Language Processing*, 2022.
- Oriane Siméoni, Huy V. Vo, Maximilian Seitzer, Federico Baldassarre, Maxime Oquab, Cijo Jose, Vasil Khalidov, Marc Szafraniec, Seungeun Yi, Michaël Ramamonjisoa, Francisco Massa, Daniel Haziza, Luca Wehrstedt, Jianyuan Wang, Timothée Darcet, Théo Moutakanni, Leonel Sentana, Claire Roberts, Andrea Vedaldi, Jamie Tolan, John Brandt, Camille Couprie, Julien Mairal, Hervé Jégou, Patrick Labatut, and Piotr Bojanowski. DINOv3, 2025.
- Stephanie Stoll, Necati Cihan Camgöz, Simon Hadfield, and Richard Bowden. Text2Sign: Towards Sign Language Production using Neural Machine Translation and Generative Adversarial Networks. *International Journal of Computer Vision (IJCV)*, 2020.
- Ilya Sutskever, Oriol Vinyals, and Quoc V Le. Sequence to sequence learning with neural networks. *Advances in neural information processing systems*, 27, 2014a.
- Ilya Sutskever, Oriol Vinyals, and Quoc V. Le. Sequence to sequence learning with neural networks, 2014b.
- Christian Szegedy, Wei Liu, Yangqing Jia, Pierre Sermanet, Scott Reed, Dragomir Anguelov, Dumitru Erhan, Vincent Vanhoucke, and Andrew Rabinovich. Going deeper with convolutions. In *2015 IEEE Conference on Computer Vision and Pattern Recognition (CVPR)*, pages 1–9, 2015.
- Shengeng Tang, Dan Guo, Richang Hong, and Meng Wang. Graph-based multimodal sequential embedding for sign language translation. *IEEE Transactions on Multimedia*, 24:4433–4445, 2022.
- Laia Tarrés, Gerard I. Gállego, Amanda Duarte, Jordi Torres, and Xavier Giró i Nieto. Sign language translation from instructional videos. In *Proceedings of the IEEE/CVF Conference on Computer Vision and Pattern Recognition (CVPR) Workshops*, 2023.
- Ashish Vaswani, Noam Shazeer, Niki Parmar, Jakob Uszkoreit, Llion Jones, Aidan N Gomez, Łukasz Kaiser, and Illia Polosukhin. Attention Is All You Need. In *Advances in Neural Information Processing Systems (NIPS)*, 2017.
- Špela Vintar, Boštjan Jerko, and Marjetka Kulovec. Compiling the slovene sign language corpus. In *5th Workshop on the Representation and Processing of Sign Languages: Interactions between Corpus and Lexicon. Language Resources and Evaluation Conference (LREC)*, pages 159–162, 2012.
- C. Vogler and D. Metaxas. Asl recognition based on a coupling between hmms and 3d motion analysis. In *Sixth International Conference on Computer Vision (IEEE Cat. No.98CH36271)*, pages 363–369, 1998.
- U. Von Agris and K.-F. Kraiss. Signum database: Video corpus for signer-independent continuous sign language recognition. In *Workshop on Representation and Processing of Sign Languages*, pages 243–246, 2010.
- Ting-Chun Wang, Ming-Yu Liu, Jun-Yan Zhu, Guilin Liu, Andrew Tao, Jan Kautz, and Bryan Catanzaro. Video-to-Video Synthesis. In *Advances in Neural Information Processing Systems (NIPS)*, 2018a.
- Ting-Chun Wang, Ming-Yu Liu, Jun-Yan Zhu, Andrew Tao, Jan Kautz, and Bryan Catanzaro. High-Resolution Image Synthesis and Semantic Manipulation with Conditional GANs. In *Proceedings of the IEEE Conference on Computer Vision and Pattern Recognition (CVPR)*, 2018b.
- Enze Xie, Wenhai Wang, Zhiding Yu, Anima Anandkumar, Jose M Alvarez, and Ping Luo. Segformer: Simple and efficient design for semantic segmentation with transformers. *Advances in Neural Information Processing Systems*, 34: 12077–12090, 2021.
- Zhenda Xie, Zheng Zhang, Yue Cao, Yutong Lin, Jianmin Bao, Zhuliang Yao, Qi Dai, and Han Hu. Simmim: A simple framework for masked image modeling. In *CVPR*, 2022.
- Zhendong Yang, Ailing Zeng, Chun Yuan, and Yu Li. Effective whole-body pose estimation with two-stages distillation. In *Proceedings of the IEEE/CVF International Conference on Computer Vision*, pages 4210–4220, 2023.
- Aoxiong Yin, Zhou Zhao, Weike Jin, Meng Zhang, Xingshan Zeng, and Xiaofei He. Mslt: Towards multilingual sign language translation. In *Proceedings of the IEEE/CVF Conference on Computer Vision and Pattern Recognition*, pages 5109–5119, 2022.
- Kayo Yin, Amit Moryossef, Julie Hochgesang, Yoav Goldberg, and Malihe Alikhani. Including signed languages in natural language processing. *Proceedings of the 59th Annual Meeting of the Association for Computational Linguistics and the 11th International Joint Conference on Natural Language Processing*, 2021.
- Jason Yosinski, Jeff Clune, Yoshua Bengio, and Hod Lipson. How transferable are features in deep neural networks?, 2014.
- Denis Zavadski, Damjan Kalšan, and Carsten Rother. Primedepth: Efficient monocular depth estimation with a stable diffusion preimage, 2024.
- Jan Zelinka and Jakub Kanis. Neural sign language synthesis: Words are our glosses. In *The IEEE Winter Conference on Applications of Computer Vision*, pages 3395–3403, 2020a.

- Jan Zelinka and Jakub Kanis. Neural Sign Language Synthesis: Words Are Our Glosses. In *The IEEE Winter Conference on Applications of Computer Vision (WACV)*, 2020b.
- Biao Zhang, Mathias Müller, and Rico Sennrich. SLTUNET: A simple unified model for sign language translation. In *The Eleventh International Conference on Learning Representations*, 2023a.
- Feihu Zhang, Jin Fang, Benjamin Wah, and Philip Torr. Deep fusionnet for point cloud semantic segmentation. In *ECCV*, 2020.
- Sen Zhang, Xiaoxiao He, Di Liu, Zhaoyang Xia, Mingyu Zhao, Chaowei Tan, Vivian Li, Bo Liu, Dimitris N. Metaxas, and Mubbasir Kapadia. Large sign language models: Toward 3d american sign language translation, 2025.
- Zhuosheng Zhang, Aston Zhang, Mu Li, Hai Zhao, George Karypis, and Alex Smola. Multimodal chain-of-thought reasoning in language models. *CoRR*, abs/2302.00923, 2023b.
- Weichao Zhao, Hezhen Hu, Wengang Zhou, Jiabin Shi, and Houqiang Li. Best: Bert pre-training for sign language recognition with coupling tokenization. In *Proceedings of the AAAI conference on artificial intelligence*, pages 3597–3605, 2023.
- Hao Zhou, Wengang Zhou, Weizhen Qi, Junfu Pu, and Houqiang Li. Improving sign language translation with monolingual data by sign back-translation. *Proceedings of the IEEE/CVF Conference on Computer Vision and Pattern Recognition (CVPR)*, pages 1316–1325, 2021a.
- Hao Zhou, Wengang Zhou, Weizhen Qi, Junfu Pu, and Houqiang Li. Improving sign language translation with monolingual data by sign back-translation. In *Proceedings of the IEEE/CVF Conference on Computer Vision and Pattern Recognition*, pages 1316–1325, 2021b.
- Hao Zhou, Wengang Zhou, Yun Zhou, and Houqiang Li. Spatial-temporal multi-cue network for sign language recognition and translation. *IEEE Transactions on Multimedia*, 24:768–779, 2021c.
- Wengang Zhou, Weichao Zhao, Hezhen Hu, Zecheng Li, and Houqiang Li. Scaling up multimodal pre-training for sign language understanding. *IEEE Transactions on Pattern Analysis and Machine Intelligence*, 2025.
- Yang Zhou, Zhaoyang Xia, Yuxiao Chen, Carol Neidle, and Dimitris N. Metaxas. A multimodal spatio-temporal GCN model with enhancements for isolated sign recognition. In *Proceedings of the LREC-COLING 2024 11th Workshop on the Representation and Processing of Sign Languages: Evaluation of Sign Language Resources*, pages 408–419, Torino, Italia, 2024. ELRA and ICCL.
- Ronglai Zuo and Brian Mak. C2slr: Consistency-enhanced continuous sign language recognition. In *CVPR*, pages 5131–5140, 2022.
- Ronglai Zuo, Fangyun Wei, and Brian Mak. Natural language-assisted sign language recognition. In *Proceedings of the IEEE/CVF conference on computer vision and pattern recognition*, pages 14890–14900, 2023.

A	Background Information	14
A.1	Sign Language Recognition	14
A.2	Pose Estimation	14
A.3	Diffusion Models	15
A.4	Vision Transformer	15
B	Methodology for Constructing Sign Language Latent Space	15
B.1	Stage 1: ViT Pose2Gloss Part Training	16
B.2	Stage 2: ViT Video2Pose Part Training	16
B.3	Implementation Details of Latent Space	17
C	More Continuous Sign Language Recognition Details	17
D	More Experimental Results	18
D.1	Evaluation Metrics	18
D.2	Training Efficiency of Constructing Compact Pose-Rich Latent Space	18
D.3	Ablation Study of Constructing Compact Pose-Rich Latent Space .	19
D.4	Qualitative Assessment	19
D.5	Inference Efficiency Assessment .	19
D.6	Ablation Assessment of Five modalities	20
D.7	Visualization and in-depth Analysis (I)	21
D.8	Visualization and in-depth Analysis (II)	21
E	Discussion	22
E.1	Integrity of Technical Implementation	22
E.2	Rigorous Benchmarking on the ASLLRP Dataset	22
E.3	Component Customization and Scalability	22
E.4	Compactness and Computational Efficiency	22
E.5	Discussion on the overall motivation and methodology	23

A Background Information

A.1 Sign Language Recognition

Sign language recognition is an important research direction, at the intersection of computer vision and natural language processing. Early works mainly relied on hand-crafted features and rules to recognize small sign language vocabularies (Grobel and

Assan, 1997; Kadir et al., 2004). Subsequently, methods based on the use of machine learning (HMMs) and 3D human pose and motion analytics were used to recognize ASL (Vogler and Metaxas, 1998; Metaxas, 1999). With the development of deep learning, neural network-based methods began to dominate this field. The earliest deep learning methods used CNN (Hershey et al., 2017) to extract spatial features from video frames and then used RNN (Sutskever et al., 2014a) to model temporal relationships (Cui et al., 2017; Koller et al., 2015b). Although these methods were simple and direct, they struggled to capture fine-grained dynamic movements (Fang et al., 2025b).

Subsequently, researchers began to introduce human pose estimation technology (Katz, 1987; Ko et al., 2019a; Charles et al., 2014; Cihan Camgöz et al., 2020; Moryossef et al., 2020; Yin et al., 2022), converting sign language videos into skeleton sequences for recognition, which significantly improved the models’ ability to perceive action details (Saunders et al., 2020b, 2021a). With the advancement of computer vision technology, various powerful pose estimation methods (Cai et al., 2023; Yang et al., 2023) have emerged. However, because of their different data formats and representation methods, finding a way to effectively integrate this heterogeneous information has become an urgent challenge (Stoll et al., 2020; Huang et al., 2021; Fang et al., 2025a,c). As shown in Table 5, different datasets focus on different output goals. Understanding also requires taking account of the complex syntax of these languages. This involves not only linear sign order, but also interactions with non-manual signals, which play an essential grammatical role in signed languages. Gloss-based representations like “I-GO-STORE” can help, in part, to model the unique linguistic rules of a given signed language (Camgöz et al., 2018; Cihan Camgöz et al., 2020; Liddell et al., 2003; Zelinka and Kanis, 2020a,b; Neidle and Ballard, 2022; Zhou et al., 2024; Neidle et al., 2022b; Zhang et al., 2025).

A.2 Pose Estimation

Pose estimation technology has made significant progress in recent years. SMPLer-X (Cai et al., 2023) achieves precise modeling of the body, hands, and face by providing complete 3D human body model parameter estimation (Loper et al., 2015; Cao et al., 2017). DWPose (Yang et al., 2023) focuses on 2D keypoint detection, achieving real-

Dataset	Duration(h)			Vocabulary(k)			Annotation Type	Year	Domain
	train	val	test	train	val	test			
KETI (Ko et al., 2019a)	20.05	2.24	5.70	←	0.49	→	Spoken Text	2019	Emergency situations
PHOENIX-2014T (Camgoz et al., 2018a)	9.2	0.6	0.7	2	0.9	1	Spoken Text, Gloss	2018	Weather Forecast
CSL Daily (Zhou et al., 2021a)	20.62	1.24	1.41	2	1.3	1.3	Spoken Text, Gloss	2021	Daily life
OpenASL (Shi et al., 2022)	←	288	→	←	33	→	Spoken Text	2022	Youtube (news + vlogs)
How2Sign (Duarte et al., 2021a)	69.6	3.9	5.6	15.6	3.2	3.6	Spoken Text	2021	Instructional
ASLLRP (Neidle et al., 2022a)	←	80	→	←	2.1	→	Gloss	2022	Comprehensive

Table 5: **Comparison of sign language datasets by annotation type and task focus:** The top five rows primarily focus on translation to spoken word text. However, our main focus is on recognition of ASL signs (identified by ID Gloss labels) from poses and sign language videos. ← → indicate that in some cases only statistics on the whole dataset are provided.

time performance while ensuring stability (Wang et al., 2018a; Lugaresi et al., 2019). Google’s MediaPipe (Lugaresi et al., 2019) provides lightweight but accurate 3D pose prediction, making real-time applications possible (Lugaresi et al., 2019; Chan et al., 2019).

Beyond traditional pose estimation, there are also emerging technologies. PrimeDepth (Zavatski et al., 2024), specifically designed for depth estimation, can provide 3D structural information about scenes (Qiu et al., 2021; Carreira and Zisserman, 2017). Sapiens segmentation (Khirodkar et al., 2024) provides a new perspective for interpreting signers’ fine-grained actions through precise human body part segmentation (Güler et al., 2018; Saunders et al., 2021b). These advances provide rich feature representation methods for SL recognition, offering good extensions to the information dimensions of pose estimation (Szegedy et al., 2015; Koller, 2020).

A.3 Diffusion Models

Diffusion models have achieved breakthroughs in the generative arena in recent years. From the initial DDPM (Ho et al., 2020) to Stable Diffusion (Rombach et al., 2021), diffusion models have demonstrated powerful image generation capabilities (Saunders et al., 2021c; Wang et al., 2018b). Researchers have also begun applying diffusion to discrete text sequence generation, with promising results (Ko et al., 2019b; Boháček and Hružík, 2022). Particularly in cross-modal conversion tasks, diffusion models have shown excellent performance, providing important references for converting SL videos to text (Saunders et al., 2020b; Cooper and Bowden, 2007; Zhou et al., 2024).

The success of the stable diffusion model lies in the fact that it conducts learning not at the pixel level but in the latent space (Fang et al., 2025d). This enables its learning to be not only smooth but

also with a reduced computational burden. Inspired by its success, our work also to apply sign language recognition in the sign latent space, and as a result, we have achieved very good results.

A.4 Vision Transformer

Since the development of ViT (Dosovitskiy et al., 2021), the use of Transformers in vision tasks has become increasingly widespread. Compared to traditional architectures, Transformers can better model long-range dependencies through self-attention mechanisms (Saunders et al., 2021a; Huang et al., 2021). The original ViT first applied pure Transformer structure to image classification, pioneering a new paradigm of vision Transformers. Subsequent improvements, such as Swin Transformer and other models, further enhanced model performance in vision tasks by introducing local attention mechanisms (Cihan Camgöz et al., 2020; Ko et al., 2019b). In the field of video event recognition, researchers have introduced spatiotemporal attention mechanisms, enabling ViT to better process video sequence data (Boháček and Hružík, 2022; Forster et al., 2012). This advance is particularly important for SL recognition, as SL videos contain rich temporal information. Through well-designed spatiotemporal attention mechanisms, models can effectively capture temporal dependencies in sequences of signing (Koller et al., 2015a; Saunders et al., 2021b).

B Methodology for Constructing Sign Language Latent Space

Dataset Preparation. Our process of constructing the rich pose latent space utilize a linguistically annotated ASL dataset of continuous signing: the ASLLRP SignStream@ 3 Corpus (Neidle et al., 2022a). This dataset contains over 80 hours of American Sign Language

(ASL) videos with synchronized front view, side view, and facial close-up recordings. These videos have been linguistically annotated using SignStream® (Neidle et al.) software (see <https://www.bu.edu/asllrp/SignStream/3/>), providing detailed manually annotated gloss labels, sign types, handshape information, and non-manual grammatical markers. The dataset comprises 2,127 utterances with 17,522 sign tokens, plus an additional set of 542 sentences from DawnSignPress.

For video processing, we apply five pose extraction models: SMPLer-X (Cai et al., 2023) for accurate 3D human body parameters, DWPose (Yang et al., 2023) for real-time 2D keypoint detection, MediaPipe (Lugaresi et al., 2019) for lightweight 3D pose prediction, PrimeDepth (Zavadski et al., 2024) for hand depth information, and Sapiens segmentation (Khirodkar et al., 2024) for fine-grained body part segmentation. Unlike previous approaches, our preprocessing strategy retains some incomplete or slightly occluded video samples to enhance model robustness to quality variations in real-world scenarios. Videos are standardized to 30fps and processed at uniform spatial resolution. We extract multimodal pose features from all videos to form a unified representation space.

Sign recognition presents significant challenges in multimodal representation learning, particularly in converting continuous visual gestures into discrete textual descriptions (Cihan Camgöz et al., 2020; Cihan Camgoz et al., 2018; Saunders et al., 2020a; Kim et al., 2022). Regarding the construction of the posture latent space, We propose a 2-stage training approach based on ViT that systematically learns Pose2Gloss and Video2Pose stages.

B.1 Stage 1: ViT Pose2Gloss Part Training

Text Generation Loss. Following seq2seq principles (Sutskever et al., 2014b), we employ a cross-entropy text generation loss (Mao et al., 2023) that measures the probabilistic divergence between predicted and ground truth token (word index in codebook) sequences:

$$L_{\text{text}} = - \sum_{i=1}^N y_{\text{true},i} \log(y_{\text{pred},i}) \quad (10)$$

where N denotes sequence length, $y_{\text{true},i}$ represents ground truth tokens, and $y_{\text{pred},i}$ represents predicted token probabilities.

Word Matching Loss. To further improve vocabulary precision and text coherence, we introduce a word matching loss $\mathcal{L}_{\text{word}}$ that directly compares predicted and ground-truth token embeddings using cosine similarity. This loss is defined as:

$$\mathcal{L}_{\text{word}} = \frac{1}{B} \sum_{b=1}^B (1 - \text{sim}(e_{\text{pred},b}, e_{\text{true},b})), \quad (11)$$

where B is the batch size, $e_{\text{pred},b}$ and $e_{\text{true},b}$ represent the embeddings of the predicted and ground-truth tokens for batch sample b , respectively, and $\text{sim}(\cdot, \cdot)$ denotes the cosine similarity function. By minimizing this loss, the model learns to align the predicted token embeddings with their true counterparts, enhancing the semantic accuracy and fluency of the generated text. This approach proves particularly effective in addressing over-long or incoherent outputs observed with the text generation loss alone.

Contrastive Learning Loss. Inspired by recent multimodal representation learning (Chen et al., 2020; Lu et al., 2023b; Zhang et al., 2023b), we introduce a contrastive alignment loss that encourages semantic proximity between pose and text embeddings:

$$L_{\text{contrast}} = - \log \frac{\exp(\text{sim}(z_{\text{pose}}, e_{\text{text}})/\tau)}{\sum_j \exp(\text{sim}(z_{\text{pose}}, e_{\text{text}}^j)/\tau)}. \quad (12)$$

The loss leverages cosine similarity between pose embeddings z_{pose} (output of moude) and text embeddings e_{text} (index of codebook), with τ as a temperature scaling parameter to control embedding separation, where $\exp(\cdot)$ denotes the exponential function.

Composite Loss Formulation. The total loss is formulated as a weighted combination of these components:

$$L_{\text{total}} = \lambda_{\text{text}} L_{\text{text}} + \lambda_{\text{word}} L_{\text{word}} + \lambda_{\text{contrast}} L_{\text{contrast}}. \quad (13)$$

B.2 Stage 2: ViT Video2Pose Part Training

Following feature transfer learning principles (Yosinski et al., 2014), we freeze the Pose2Gloss module and train the Video2Pose component by minimizing the reconstruction error:

$$L_{\text{video2pose}} = \sum_i \|\hat{P}_i - P_i\|^2, \quad (14)$$

Config	Stage 1 (Pose2Gloss)	Stage 2 (Video2Pose)
optimizer	AdamW	AdamW
base learning rate	1×10^{-3}	1×10^{-3}
weight decay	0.01	0.01
optimizer momentum	$\beta_1 = 0.9, \beta_2 = 0.999$	$\beta_1 = 0.9, \beta_2 = 0.999$
learning rate schedule	Cosine decay (min = $0.05 \times lr$)	Cosine decay (min = $0.01 \times lr$)
warmup steps	Dynamic (2%-10% of total steps)	10% of total steps
training epochs	500-1000	300
batch size	32	32
gradient accumulation	4	0
gradient clipping	7.0	1.0
label smoothing	0.1	N/A
teacher forcing ratio	Decay from 0.5 to 0	N/A
text loss weight	1	1
word match weight	1	N/A
contrast loss weight	1	N/A
max sequence length	64	64
temperature	0.7 (inference)	0.7 (inference)
beam size	5 (inference)	5 (inference)
length penalty	0.7 (inference)	0.7 (inference)
top-k	50 (sampling)	50 (sampling)
top-p	0.92 (sampling)	N/A
repetition penalty	2.5 (beam search)	N/A

Table 6: **Comprehensive training configurations and hyperparameters:** Optimizer settings, learning schedules, training parameters, and inference configurations for both stages.

where \hat{P}_i represents predicted pose representations and P_i denotes ground truth pose representations. This 2-stage approach enables specialized learning for each module, creating a robust sign recognition system that effectively bridges visual and textual domains.

B.3 Implementation Details of Latent Space

For Stages 1 and 2, we use the linguistically annotated ASLLRP SignStream® 3 Corpus of continuous signing (Neidle et al., 2022a) as primary datasets for American Sign Language (ASL) recognition. During Stage 1, we initially found that the heterogeneity and varying formats of pose features from diverse sources had a significant negative impact on the structural integrity of our latent space. To address this, we prioritized optimizing the cross-modal alignment and feature consistency in the Pose2Gloss module (Stage 1) through a gloss-aware latent distillation loss. However, we observed that relying solely on feature-level distillation did not sufficiently address the nuances of sign-to-text generation quality.

We explored text generation using a cross-entropy loss $\mathcal{L}_{\text{text}}$. While this approach improved basic text output, it frequently generated over-long and incoherent text, limiting practical utility. To address this, we investigated an n-gram consistency loss designed to balance precision and recall, but found this implicit matching approach less effective than directly focusing on vocabulary alignment. We therefore introduced a word matching loss that measures cosine similarity between predicted and

ground-truth token embeddings, encouraging precise vocabulary generation within our custom CodeBook. Additionally, we incorporated contrastive learning with temperature parameter τ to further encourage semantic proximity between the ViT-constructed pose latent space and text representations.

For Stage 2 (Video2Pose), we froze the Pose2Gloss parameters trained in Stage 1 and developed a Vision Transformer-based model to convert raw video inputs directly into the unified pose latent representation, minimizing the reconstruction loss $\mathcal{L}_{\text{video2pose}} = \sum_i \|\hat{P}_i - P_i\|^2$, where \hat{P}_i represents predicted latent pose representations and P_i denotes ground-truth unified poses. This 2-stage approach, leveraging the pre-trained ViT latent space, ensures robust video-to-pose conversion while maintaining evaluation efficiency. These optimizations, combined with gradient accumulation, as detailed in Table 6, resolved initial training instability and enhanced model performance. The best options for weights, pose types, and temperature values for different losses were determined through extensive ablation experiments.

C More Continuous Sign Language Recognition Details

Hybrid Temporal Modeling. The distilled latent sequences feed a hybrid backbone that remains modality-agnostic. First, a *multi-scale Temporal-Conv stack* captures hierarchical temporal patterns through parallel 1D convolutions with kernel sizes $\mathcal{K} = \{3, 5, 7\}$, corresponding to short-term (3 frames $\approx 0.1s$), medium-term (5 frames $\approx 0.17s$), and long-term (7 frames $\approx 0.23s$) dependencies. Each branch applies:

$$h_t^{(k)} = \text{MaxPool}(\text{ReLU}(\text{BN}(\text{Conv1D}_k(z_t))))),$$

$$k \in \mathcal{K} \tag{15}$$

where stride-2 pooling progressively compresses the sequence from T to $T' \approx T/4$. The outputs are concatenated and projected to $h_t \in \mathbb{R}^{1024}$. These features then pass through a bidirectional LSTM (2 layers, hidden size 512 per direction) to capture long-range dependencies, yielding $u_t \in \mathbb{R}^{1024}$. This design mirrors the receptive field hierarchy in human visual processing, where ASL comprehension relies on both rapid hand movements and sustained body postures.

D More Experimental Results

D.1 Evaluation Metrics

For sign recognition, we measure:

1. Word Error Rate (WER): As the standard metric for Continuous Sign Language Recognition (CSLR), WER quantifies the alignment between the predicted gloss sequence and the ground truth by calculating the normalized edit distance:

$$\text{WER} = \frac{S + D + I}{N} \quad (16)$$

where S , D , and I represent the number of *substitutions*, *deletions*, and *insertions* required to transform the hypothesis into the reference, respectively. N denotes the total number of glosses in the reference. A lower WER indicates higher recognition stability, particularly in capturing the subtle transitions between sign gestures.

2. BLEU-n Score: To evaluate the translation quality of the generated glosses or sentences, we employ the BLEU score, which measures the n -gram precision between the candidate and reference sequences:

$$\text{BLEU} = \text{BP} \cdot \exp \left(\sum_{n=1}^k w_n \ln p_n \right) \quad (17)$$

Here, p_n denotes the modified n -gram precision, and w_n represents the uniform weight $1/k$. The Brevity Penalty (BP) is incorporated to penalize overly short predictions:

$$\text{BP} = \begin{cases} 1 & \text{if } c > r \\ e^{(1-r/c)} & \text{if } c \leq r \end{cases} \quad (18)$$

where c is the length of the candidate and r is the reference length. Higher BLEU scores reflect better semantic consistency and linguistic fluency of the SignX decoder.

3. Per-Instance (P-I) Top-1 Accuracy: Per-instance (P-I) accuracy is the primary metric used to evaluate the overall recognition performance of SignX across the entire test set. It treats each video sample as an independent and equal evaluation unit, representing the global classification accuracy (Micro-average). Formally, it is defined as:

$$\text{Acc}_{P-I} = \frac{\sum_{i=1}^C n_{i,i}}{\sum_{i=1}^C N_i} \quad (19)$$

where C denotes the total number of sign categories in the dataset (e.g., 2,000 for WLASL2000), $n_{i,i}$

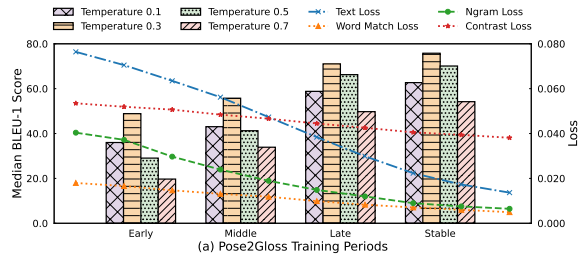


Figure 5: **Optimization efficiency in constructing the pose-rich latent space.** This figure tracks the convergence of four critical loss components designed to shape the latent space. The synchronized decline of Text and Word Match losses demonstrates the successful encoding of sign semantics into the unified latent representation.

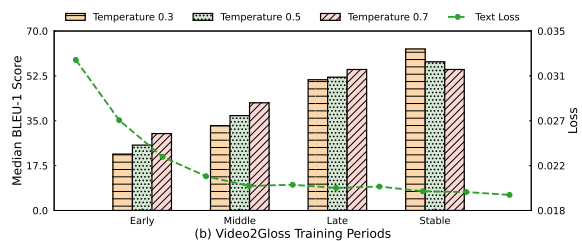


Figure 6: **Impact of hyperparameter settings on latent space quality.** We evaluate how temperature variations affect the discriminative power of the constructed latent space across different optimization periods. The results highlight the necessity of balancing generation precision and representation stability to maintain a compact pose-rich encoding.

is the number of samples from class i correctly identified by the model, and N_i is the total number of test samples belonging to category i .

D.2 Training Efficiency of Constructing Compact Pose-Rich Latent Space

The efficiency of constructing our pose-rich latent space is quantitatively analyzed in Fig. 5, which monitors the progression of four specialized loss objectives: Text Loss, Word Match Loss, Ngram Loss, and Contrast Loss. The line plots illustrate a consistent downward trend in Text and Word Match losses, confirming that the latent space is effectively learning to accommodate high-dimensional pose information while maintaining precise semantic mappings. The stabilization of Ngram Loss and the controlled trajectory of Contrast Loss further indicate that the space is achieving structural coherence, ensuring that heterogeneous pose features are harmonized into a compact, information-dense representation.

Phoenix-14T (German Sign Language)
<p><i>Generated Text:</i> ES-BEDEUTET HERBST WOLKE UND UND KOENNEN GEWITTER</p> <p><i>English:</i> It means autumn cloud and and can thunderstorm</p> <p><i>Ground Truth:</i> ES-BEDEUTET VIEL WOLKE UND KOENNEN REGEN GEWITTER KOENNEN</p> <p><i>English:</i> That means lots of clouds and again and again strong showers and thunderstorms</p>
<p><i>Generated Text:</i> TAG DANN SUED SUEDOST NACH MITTAG IX NOVEMBER GEWITTER</p> <p><i>English:</i> Day then south southeast after midday IX November thunderstorm</p> <p><i>Ground Truth:</i> TAG DANN SUED SUEDOST REGEN NACH MITTAG IX AUCH GEWITTER</p> <p><i>English:</i> During the day it rains in the south and south-east, and in the afternoon there are also local thunderstorms</p>
CSL-Daily (Chinese Sign Language)
<p><i>Generated Text:</i> 这 这考虑 画画 是 自己 仔细 方法 分析</p> <p><i>English:</i> This, this, consider painting is one's own careful method analysis</p> <p><i>Ground Truth:</i> 这 画画 是 他 自己 努力 仔细 想 方法 结果</p> <p><i>English:</i> This painting is the result of his own hard work and careful thinking</p>
<p><i>Generated Text:</i> 不管 结果 情况 情况 大概 努力</p> <p><i>English:</i> No matter the result, the situation, the situation, or the effort</p> <p><i>Ground Truth:</i> 不管 结果 情况 我 一直 努力</p> <p><i>English:</i> No matter the result or situation, I will always work hard</p>

Table 7: **Qualitative evaluation of sign language translation.** The examples demonstrate the model’s generalization capability across diverse sign languages (German and Chinese).

D.3 Ablation Study of Constructing Compact Pose-Rich Latent Space

To further refine the properties of the constructed latent space, we conducted an ablation study on the temperature settings, as shown in Fig. 6. We examined the BLEU scores across four temperature levels (0.1, 0.3, 0.5, and 0.7) to determine the optimal configuration for latent space stability and gloss accuracy. The evaluation across early to stable periods reveals that a moderate temperature of 0.3 facilitates the most robust latent representation for sign recognition. We observed that while initial space formation benefits from this moderate setting, the subsequent refinement of the video-to-latent mapping favors lower temperatures to enhance precision. This balance is crucial for ensuring that the latent space remains both expressive and discriminative. Through this optimization, we also established the final weighting scheme for the latent space loss functions.

D.4 Qualitative Assessment

As illustrated in Table 7, the model demonstrates robust performance across both weather broadcast (Phoenix-14T) and daily conversation (CSL-Daily) domains. In the Phoenix-14T examples, the model successfully captures the core semantic content of weather forecasts. In the first example, key meteorological terms like “WOLKE” (cloud) and “GEWITTER” (thunderstorm) are accurately

Method	FPS \uparrow	Power (W) \downarrow	WER (%) \downarrow
Transformer + Visual Encoder	0.05	26.22	43.26
SignX (CSLR in Pixel Space)	0.57	29.20	32.78
SignX (CSLR in Latent Space)	2.42	24.58	26.59

Table 8: **Inference Efficiency on ASLLRP:** SignX achieves faster performance by operating in latent space, during the 800-step training process.

predicted, though with minor lexical substitutions (e.g., “HERBST” for “VIEL”). The second example shows the model’s ability to preserve temporal markers (“NACH MITTAG”) and directional information (“SUED SUEDOST”), while occasionally omitting modifiers like “AUCH” (also) and “REGEN” (rain). For CSL-Daily, the model exhibits strong semantic preservation despite surface-level variations. The first example accurately conveys the relationship between artistic creation and effort, with key concepts like “画画” (painting), “仔细” (careful), and “方法” (method) correctly identified. The second example demonstrates the model’s capability in handling abstract concepts, where “不管” (no matter) and “努力” (effort) are preserved, though with slight word duplication (“情况 情况”) that does not significantly impair comprehension. These results indicate that our approach effectively maintains semantic coherence across diverse sign language contexts, though there remains room for improvement in handling function words and fine-grained temporal/spatial modifiers.

D.5 Inference Efficiency Assessment

Table 8 presents a comparative analysis of inference efficiency and recognition performance on the ASLLRP dataset. The results demonstrate the clear superiority of the proposed **SignX (CSLR in Latent Space)** across all evaluated metrics. Notably, the latent space variant achieves an inference speed of **2.42 FPS**, representing an approximately $4.2\times$ speedup over its pixel-space counterpart (0.57 FPS) and nearly a 50-fold acceleration compared to the baseline **Transformer + Visual Encoder** (0.05 FPS).

Beyond throughput, our latent space approach exhibits the highest energy efficiency with a power consumption of **24.58 W**, whereas the pixel-space model incurs a higher overhead of 29.20 W. Crucially, this gain in efficiency does not come at the cost of accuracy; SignX in latent space yields the lowest WER of **26.59%**, marking a significant improvement over the baseline’s 43.26%. These find-

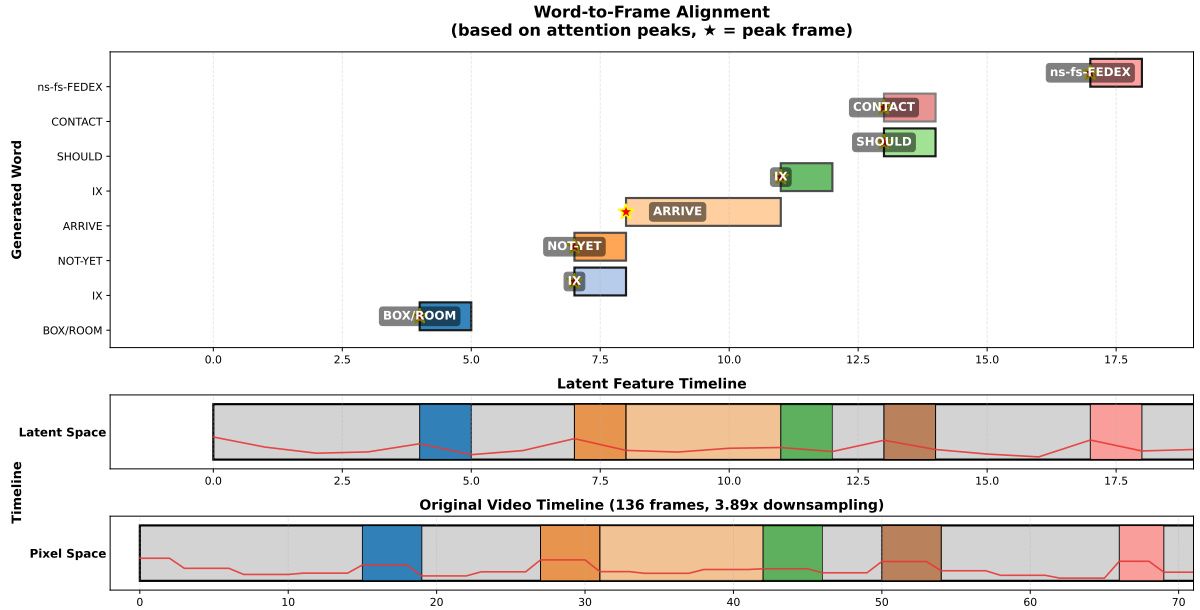


Figure 7: **Attention Analysis.** Here, we have analyzed the feature extraction and recognition section. The above figure represents the analyzed Gloss for different potential representations. Each representation is derived from 5 to 10 frames. This area represents the relative position of this representation. The two progress bars below represent the relative positions at the feature level and the pixel frame level respectively. The red line is the intensity of attention.

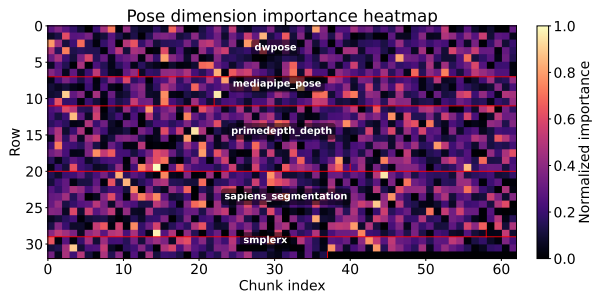


Figure 8: **Importance Visualization of different modalities.** Normalized importance heatmap of 1959 pose feature dimensions across five pose types, separated by red boundary lines. Warmer colors indicate higher activation importance.

ings validate that operating within a compact, pose-rich latent space effectively mitigates the computational burden of high-dimensional video processing while simultaneously enhancing the robustness of continuous sign language recognition.

D.6 Ablation Assessment of Five modalities

As shown in Figure 8, during the extraction process of Video2Pose, we analyzed the attention intensities of different dimensions. We can observe that the intensities of different dimensions of the ViT used for accommodating the creation of the Latent Space after training are very evenly distributed. Therefore, we can conclude that during the main stage where it plays a role, all the postures have similar levels of importance.

Table 9 summarizes a further, more granular as-

Ablated Modality (Zeroed)	WER (%)	Δ WER	Relative Degradation
SignX (Full Pipeline)	26.59	–	–
w/o SMPLeR-X	29.65	+3.06	11.51%
w/o DWPose	32.31	+5.72	21.51%
w/o MediaPipe	29.37	+2.78	10.46%
w/o PrimeDepth	30.89	+4.30	16.17%
w/o Sapiens	30.53	+3.94	14.82%

Table 9: **Ablation assessment of different modalities:**

For each modality mentioned in the first column, the corresponding output is set to zero during video processing. Recognition is then performed within the corrupted latent space to observe the impact on model performance. The Full Pipeline model is a Vid2Pose module trained for 30 epochs. Upon zeroing a modality, the CSLR model is fine-tuned for 1,000 steps within the resulting corrupted latent space before performance comparison.

assessment of modality ablation, in which specific modality outputs are zeroed to generate various corrupted versions of the latent space for a detailed analysis of each modality’s contribution to the overall framework. We perform restorative training within these corrupted spaces to observe the impact of missing modalities on downstream recognition, moving beyond the evaluation of the initial extraction pipeline. As illustrated in the table, DW-Pose and depth information exert the most significant influence on performance, which aligns with the conventional consensus that these two types of data are paramount for sign language recognition. The lowest impact is observed from MediaPipe Pose, which we hypothesize is because its functional role is largely subsumed by the supe-

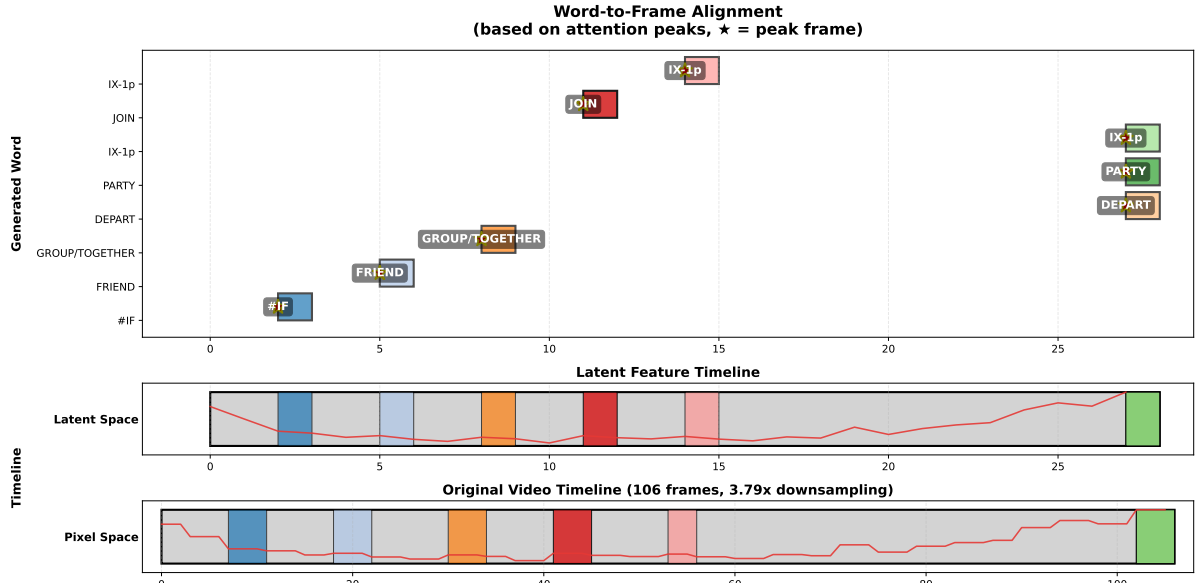


Figure 9: **Further analysis of the reasons for excellence.** To verify the entire pipeline of our model for the CSLR process and understand how its mechanism operates, we selected a sample in the translation process where all video features were concentrated at the relatively tail end. In this sample, the last video feature encoded information about three postures.

rior precision of DWPose. Notably, although we performed 1,000 steps of additional restorative fine-tuning for each configuration, the aggregate performance degradation remains relatively controlled. This phenomenon indicates that a substantial portion of linguistic information is shared across different modalities, thereby validating our original motivation for constructing a compact and highly compressed latent space .

D.7 Visualization and in-depth Analysis (I)

To analyze the internal mechanics of our model, we visualize the temporal alignment in Figure 7. In our framework, one latent feature typically contains information from approximately 5 to 10 video frames. Consequently, a single gloss is often represented by only one or two features.

As shown in the three-layer alignment (Gloss \leftrightarrow Feature Index \leftrightarrow Original Frames), we observe a key phenomenon: even a single feature can be identified with multiple meanings. For example, **Peak Feature 6** is simultaneously mapped to the glosses *IX* and *NOT-YET*. This proves that even when the data is compressed into a single latent variable, it still retains highly useful and multifaceted information. This high information density allows the model to maintain accurate recognition while significantly reducing the computational burden.

Furthermore, for this overlapping situation, we have found that our Latent CSLR model can actually restore the chronological order of them. There

are two possible scenarios. One is that even in the Latent space, the information represented has a hidden sequence. The other is that the Latent CSLR model restored this sequence relationship. Regardless of which situation it is, it demonstrates the excellence of our model. We can further analyze in Section D.8 to determine which scenario it is.

D.8 Visualization and in-depth Analysis (II)

In the previous section, we discovered that our Latent Space (Vid2Pose) possesses excellent compression capabilities, where a single feature can represent multiple pose details. However, it remained unclear whether this success was because temporal information was recorded during compression or if the Latent CSLR restored the temporal information during translation.

Therefore, in Figure 9, we provide a sample where the features are primarily distributed at the end of the video. In this case, three glosses are output by the model only after it has finished viewing the video. We surprisingly found that this represents two major advantages of our model:

1. **Thinking-based Compression:** When Video2Pose provides features, it confirms and outputs them only after seeing the full video if it cannot determine them immediately. **Furthermore**, as the video nears its end, the level of attention begins to increase, which is also evidence that the model has thought

through and provided the video’s features after careful consideration.

2. **Contextual Restoration:** Once our Latent CSLR obtains these features, it restores them to their correct temporal positions. **For example**, the final output of the model is “#IF FRIEND GROUP/TOGETHER DEPART PARTY IX-1p JOIN IX-1p”, while the correct answer is “#IF FRIEND GROUP/TOGETHER GO-OUT PARTY IX-1p JOIN IX-1p”. We can observe that after careful consideration, the feature "PARTY", which was initially determined later, was successfully returned to its correct position. This is a remarkable ability. Although there was a spelling mistake in one word, it was not caused by our innovative approach, but rather due to the insufficient capabilities of the existing ViT.

This suggests that the model effectively internalizes a temporal realignment mechanism during the optimization process, enabling it to compensate for feature manifestation latency and accurately restore the objective chronological sequence. Based on these two experiments, we now know **why our model is excellent** (intelligent, “thinking” compression) and **where it excels** (the Latent CSLR translates by combining context). **We have discovered the reason for this success**—learning from feature post-positioning during training—and validated the future prospects and superiority of our model.

E Discussion

Here we discuss some common issues:

E.1 Integrity of Technical Implementation

The technical details described in Section 3, such as adaptive feature pruning and latent space organization, serve as the foundational implementation of our Latent CSLR framework. These components are not disjointed tricks; rather, they have been validated as a holistic system in our ablation studies (As shown in Fig. 4, 5, 6, 8 and Table. 9) to ensure the structural integrity of the latent space.

E.2 Rigorous Benchmarking on the ASLLRP Dataset

As ASLLRP is a relatively new dataset for the CSLR task, there is a lack of publicly available

baseline results from modern models. To ensure a fair comparison under identical pose input conditions, we re-implemented and fine-tuned several representative state-of-the-art (SOTA) frameworks, including SLTUNET (Zhang et al., 2023a) and C2SLR (Zuo and Mak, 2022). Our selection criteria prioritized mainstream methods that represent established technical trajectories in sign language understanding, rather than solely focusing on the most recent publication dates.

E.3 Component Customization and Scalability

All architectural components in SignX have been deeply modified to serve the objective of latent space recognition. For instance, our Custom CodeBook is utilized to learn and initialize pose-rich features beneficial for linguistic mapping. This design is inherently scalable to an unlimited vocabulary and does not restrict the model’s capacity for future expansion. Furthermore, while our framework utilizes a comprehensive set of modalities, these modules are highly reusable across different datasets. Compared to ultra-large-scale models such as Uni-Sign (Li et al., 2025), our approach achieves superior performance with a smaller data footprint, demonstrating a data-frugal and efficient research path.

E.4 Compactness and Computational Efficiency

The compactness of our latent space has been strictly validated through ablation evaluations (As shown in Fig. 4, 5, 6, 8 and Table. 9). Our compression is measured against the original raw video frame dimensionality of 150,528 ($224 \times 224 \times 3$). Through adaptive feature pruning, we successfully stabilize the latent width at approximately 1024 (The initial dimension after padding is 2048, and after pruning, compression and organization, it becomes 1024.), achieving a compression ratio exceeding $140x^3$. This significant reduction effectively mitigates computational overhead while maintaining high information density, as substantiated by our inference efficiency analysis showing a 50-fold acceleration compared to traditional pixel-space baselines (As shown in Table 8).

³Considering that multiple frames are compressed into one feature, our effective compression rate will be even higher. More importantly, after we have completed the training, we no longer need the posture extraction data preprocessing tool. In the long run, this saves a lot of time for learning posture information.

E.5 Discussion on the overall motivation and methodology

Overall, our key insight is that not only should we perform generation tasks in the Latent Space, but we should also perform recognition tasks in the Latent Space. This was deemed successful by the experiments. Initially, we had the option of using pre-trained components such as VAE (Kingma and Welling, 2013; Dong et al., 2022) and DINO3 (Siméoni et al., 2025) as alternatives, but they lacked pose-level information, lacked effective sign language semantic information, and the simple CNN in VAE could not meet our needs for scalability and stability. Therefore, after careful consideration, we adopted the existing methods. In the future, we will make more resources available, such as code and preprocessed data, to support the sign language research community.